AhR ligands from LGG metabolites promote piglet intestinal ILC3 activation and IL-22 secretion to inhibit PEDV infection

Junhong Wang[1], Yibo Zhao[1], Tong Cui[1], Hongyu Bao[1], Ming Gao[1], Mingyang Cheng[1], Yu Sun[1], Yiyuan Lu[1], Jiayao Guan[1], Di Zhang[1], Yanlong Jiang[1], Haibin Huang[1], Chunwei Shi[1], Jianzhong Wang[1], Nan Wang[1], Jingtao Hu[1], Wentao Yang[1], Guilian Yang[1], Yan Zeng[1]*, Chunfeng Wang[1]*, Xin Cao[1]*.

[1] College of Veterinary Medicine, Jilin Provincial Engineering Research Center of Animal Probiotics, Jilin Provincial Key Laboratory of Animal Microecology and Healthy Breeding, Engineering Research Center of Microecological Vaccines (Drugs) for Major Animal Diseases, Ministry of Education, Jilin Agricultural University, Changchun, 130118, China.

***Correspondence:** zengyan@jlau.edu.cn; wangchunfeng@jlau.edu.cn; xinc@jlau.edu.cn

Competing Interests statement

The authors declare that the research was conducted without any commercial or financial relationships.

Abstract

In maintaining organismal homeostasis, gut immunity plays a crucial role. The coordination between the microbiota and the immune system through bidirectional interactions regulates the impact of microorganisms on the host. Our research focused on understanding the relationship between substantial changes in jejunal intestinal flora and metabolites and intestinal immunity during porcine epidemic diarrhea virus (PEDV) infection in piglets. We discovered that *Lactobacillus rhamnosus GG* (*LGG*) could effectively prevent PEDV infection in piglets. Further investigation revealed that *LGG* metabolites interact with type 3 innate lymphoid cells (ILC3) in the jejunum of piglets through the aryl hydrocarbon receptor (AhR). This interaction promotes the activation of ILC3 cells and the production of interleukin-22 (IL-22). Subsequently, IL-22 facilitates the proliferation of IPEC-J2 cells and activates the STAT3 signaling pathway, thereby preventing PEDV infection. Moreover, the AhR receptor exerts its influence on various cell types within organoids, including intestinal stem cells (ISCs), Paneth cells, and enterocytes, fostering their growth and development, suggesting a broad impact of AhR on intestinal health. In conclusion, our study demonstrates the ability of *LGG* to modulate intestinal immunity and effectively prevent PEDV infection in piglets. These findings highlight the potential application of *LGG* as a preventive measure against viral infections in livestock.

Keywords: PEDV, ILC3, *LGG*, AhR, intestine.

Introduction

Porcine epidemic diarrhea virus (PEDV), a member of the genus Coronavirus A of the family Coronaviridae, causes acute diarrhea and/or vomiting, dehydration, and high mortality in neonatal piglets (Jung and Saif 2015). Related studies have reported significant changes in the intestinal microbiota of *Lactobacillus*, *Escherichia coli*, and *Lactococcus* in piglets as a result of PEDV infection (Yang et al., 2020a). Specifically, the abundance of *Lactobacillus* jejuni and *Lactobacillus* cecum showed a decreasing trend in PEDV-infected piglets, accompanied by significant changes in metabolites(Li et al., 2022).

In recent years, it has been found that intestinal immunity has an important role in organismal homeostasis (Yu et al., 2022). Bidirectional interactions between the microbiota and the immune system coordinate many microbial effects on the host (Ronan et al., 2021). Innate lymphoid cells (ILCs), which are continuously interacting with commensal flora in the gut, are the pioneers (Gury-BenAri et al., 2016). Meanwhile, IL-22 production by ILC is critical for intestinal immunity during the early course of infection development (Satoh-Takayama et al., 2008). Previous studies have shown that intestinal flora is a key factor in IL-22 production in the gut, but the regulatory mechanisms are unclear (Yang et al., 2020b).

In addition to interacting with a variety of intestinal epithelial cells, ILCs also interact with intestinal stem cells (ISCs) in the crypts to regulate the differentiation and function of ISCs (Lindemans et al., 2015). ILC3-derived IL-22 can promote the phosphorylation of signal transducer and activator of transcription 3 (STAT3) on

intestinal stem cells through the action of IL-22R, thus inhibiting the apoptosis of intestinal stem cells. At the same time, IL-22 can stimulate the proliferation of intestinal stem cells and then ameliorate the damage to ISCs caused by chemotherapy (Hanash et al., 2012; Aparicio-Domingo et al., 2015).

Aryl hydrocarbon receptor (AhR) is essential for the maintenance of ILC3 and the production of IL-22 (Pernomian et al., 2020). AhR is another key transcription factor for ILC3, and the presence of lymphoid tissue in the intestine is associated with intact AhR expression (Xia et al., 2017). In contrast, the removal of AhR is equivalent to the absence of ILC3, resulting in the disappearance of intestinal lymphoid tissue (Kiss et al., 2011). AhR is expressed in many mammalian tissues, particularly in the liver, intestine, and kidney. In the intestine, AhR, expressed mainly by epithelial cells and innate immune cells, plays an important role in the regulation of innate immunity and regulates the number of lymphocytes within the epithelium. When the energy source is converted from sugar to tryptophan, *Lactobacillus* lactis amplifies and produces indole-3-aldehyde (I3A), which serves as an AhR ligand that promotes the production of IL-22 by ILC3 (Zelante et al., 2013). IL-22 plays a central role in the protection of host cells against pathogens at the surface of the mucosa through the activation of STAT3 (Backert et al., 2014). It has been reported that mature IL-22 of porcine origin inhibits PEDV infection and promotes the expression of antimicrobial peptide β-defensins, cytokine IL-18, and IFN-λ through activation of the STAT3 signaling pathway (Xue et al., 2017).

An important way in which probiotics combat diarrheal diseases is by

modulating the mucosal immune system of the host intestine. Mucosal immunity is one of the important components of the body's immune system, and its main function is to remove pathogenic microorganisms that invade the body through mucosal surfaces. The mucosal immune system has a unique organizational structure and function. It is widely distributed in the mucosal tissues of the respiratory, digestive, and genitourinary tracts, serving as the main site of local immune response. The mucosal immune system consists of various components, including mucosal epithelial tissue, mucosal-associated lymphoid tissue (MALT), intestinal epithelial cells, immune cells, and the molecules or secretions they produce.

Additionally, it includes mucosal microorganisms, such as commensal microorganisms, which normally inhabit the mucosa. Some studies have reported that oral administration of *Lactobacillus* inhibits PEDV infection (Yang et al., 2023). Colonization of mice with the model probiotic *Lactobacillus rhamnosus GG* (*LGG*) enhances the maturation of intestinal function and the production of IgA and produces promising results in protection against intestinal injury and inflammation (Yan et al., 2017).

In this study, a co-culture system of porcine jejunal gut tract-like organoids with porcine jejunal lamina propria lymphocytes (LPLs) was established to examine and validate the protective effect of *Lactobacilli* on intestinal epithelial cells. Our hypothesis suggests that *LGG* may secrete substances, such as I3A, which can activate the AhR receptors located on the surface of ILC3 present in the lamina propria of the pig intestinal mucosa. This activation could potentially enhance the secretion of IL-22

by ILC3. Then, the STAT3 signaling pathway of intestinal epithelial cells was activated, regeneration of ISCs was induced to perform damage repair function, Paneth cells were induced to secrete Reg3b and Reg3g to inhibit the growth of pathogenic bacteria, and intestinal cells were induced to secrete IFN-λ to inhibit PEDV replication.

Materials and Methods

Animals and sample collection

We used 3-day-old SPF piglets, which were purchased from the Harbin Veterinary Research Institute. All piglets were transported in enclosed carts designed for SPF conditions. We collected samples from the jejunum and other tissues of the piglets. Then, we analyzed the immune cells in the jejunal tissues using flow cytometry, processed and analyzed the samples using q-PCR and other experimental methods, and sectioned and stained the tissue samples. All animal experiments complied with the requirements of the Animal Management and Ethics Committee of Jilin Agricultural University.

Cell separation

Cell samples obtained from the jejunum of piglets were subjected to subsequent flow assay and in vitro cell culture and q-PCR. Firstly, after euthanasia of piglets, about 5 cm of jejunum was dissected longitudinally, rinsed with PBS and divided into 1 cm sized intestinal fragments, which were then transferred to the separation solution (15 mL of RPMI-1640, 1% penicillin and streptomycin, 1% HEPES, 5 mM EDTA, 2

mM DTT, and 2% heat-inactivated fetal bovine serum (FBS)) and incubated for 28 minutes in a shaking incubator at 37°C and 200 rpm, and then removed. After incubation for 28 minutes in a shaking incubator at 37°C and 250 rpm, the intestinal fragments were obtained rinsed and continued into the enzyme digestion solution (8 mL RPMI-1640 medium, 1% penicillin and streptomycin, 1% HEPES, 50 mg collagenase IV, 1 mg DNase I, and 2% FBS), and incubated for 28 minutes in a shaking incubator at 37°C and 250 rpm before being removed, and then filtered through a 70-μm cell strainer to get the LPL cells in the jejunum of piglets.

Antibody Information

Invitrogen: CD2 Monoclonal Antibody (14-0029-82), CD3e Monoclonal Antibody (MA5-28774), CD3e Monoclonal Antibody (Biotin) (MA5-28771), CD11b Monoclonal Antibody (MA5-16604), CD11c Monoclonal Antibody (APC) (17-0116-42), CD21 Monoclonal Antibody (A1-19243), CD21 Monoclonal Antibody (PE) (MA1-19754), CD45 Monoclonal Antibody (FITC) (MA5-28383), CD117 (c-Kit) Monoclonal Antibody (APC) (17-1171-82), CD163 Monoclonal Antibody (PE) (MA5-16476), CD172a Monoclonal Antibody (MA5-28299), CD335 (NKp46/NCR1) Monoclonal Antibody (PE) (MA5-28352), SLA Class II DR Monoclonal Antibody (MA5-28503), Gata-3 Monoclonal Antibody (PE-Cyanine7) (25-9966-42), T-bet Monoclonal Antibody (PE) (12-5825-82), Goat anti-Mouse IgG H&L (PE- Cyanine5) (M35018).

BD Pharmingen: Fixable Viability Stain 780 (565388), Purified Rat Anti-Mouse CD16/CD32 (Mouse BD Fc Block) (553142), Rat Anti-Pig γδ T Lymphocytes (PE)

(551543), Rat Anti-Pig γδ T Lymphocytes (561486), Mouse anti-GATA3 (558686).

Abcam: Streptavidin protein (Alexa Fluor 594) (ab272189), Streptavidin protein (APC) (ab243099), Goat Anti-Mouse IgG H&L (FITC) (ab6785), Goat Anti-Rabbit IgG H&L (Alexa Fluor 488) (ab150077), Goat Anti-Mouse IgG H&L (Alexa Fluor 488) (ab150113), Goat Anti-Rat IgG H&L (Alexa Fluor 488) (ab150165), Goat F(ab')2 Anti-Mouse IgG H&L (PE) (ab7002), Goat F(ab')2 Anti-Rat IgG H&L (PE-Cyanine5) (ab130803), Goat Anti-Mouse IgG H &L (Alexa Fluor 647) (ab150115), Rabbit Anti-Goat IgG H&L (Alexa Fluor 488) (ab150141), Rat Anti-Mouse IgG1 H&L (PE) (ab99605). Anti-Villin antibody (ab244292). Anti-EpCAM antibody(ab71916). Anti-EpCAM antibody(ab71916). Anti-Ki-67 antibody(ab15580). Anti-LGR5 antibody(ab273092).

Solarbio: CFSE (S1076), PMA (P6741), D-PBS (D1040), PBS (P1010)

GE Healthcare: Percoll (17089101).

R&D: APC Anti pig IL-4 (1644057).

Sigma: Penicillin And Streptomycin (V900929), Collagenase IV (V900893-1G), Ionomycin (56092-81-0), DNase I (10104159001), DTT (3483-12-3), HEPES (H3375), EDTA (E8008), FBS (F8318).

PE Goat anti Mouse(SPP101), FITC Rabbit anti Goat (SPP101-100), PE anti Mouse (SHP501) purchased from 4A Biotech.,Ltd.

Preparation of IL-22 protein and IL-22 monoclonal antibody

The porcine IL-22 (Gene ID: 595104) gene was synthesized by consulting NCBI, and the structural domains and were examined to determine the protein expression

178 scheme, and the prokaryotic and eukaryotic expression vectors were prepared, and the
179 IL-22 protein was obtained after the prokaryotic expression was purified, and the
180 IL-22 protein was immunized to the mice and then taken from the B-cells for the
181 fusion of hybridoma cells, and large quantities of monoclonal antibodies were
182 prepared by means of ascites preparation. A large number of monoclonal antibodies
183 were prepared by ascites preparation, and the antibodies were labeled with antibody
184 labeling kit (ab201795) after purification. This part of the work was done with the
185 help of Shanghai Company.

186 **LGG and EVs Acquisition**

187 LGG (ATCC 53103) was grown in De Man, Rogosa, and Sharpe (MRS) broth
188 for 12 h at 37°C. After culturing overnight, the bacteria were inoculated 1:100 in fresh
189 MRS broth and grown under anaerobic conditions until reaching the mid-log phase.
190 Then, the colonies were counted, and the cell density was adjusted to 5×10^9
191 colony-forming units (CFU)/mL.

192 The culture was centrifuged overnight at 7,000 g for 30 min to eliminate debris,
193 including dead cells and other waste products. The supernatant obtained was filtered
194 and ultracentrifuged at 150,000g for 70 min. The precipitate was collected after
195 centrifugation (LGG-EVs were mainly enriched in the precipitate, with minimal
196 presence in the supernatant) and stored at -80°C for later use.

197 **The PEDV information**

198 The PEDV strain (PEDV LJX01/2014, PEDV N gene GenBank number:
199 MK252703) was provided by the Professor Guangliang Liu, Lanzhou Veterinary

Research Institute, China. The propagation and titration of the PEDV LJX strain were described previously (Chen et al., 2020). Piglets were infected by oral feeding using a virus with a copy number of 1.35×10^4 RNA copies/g, and each piglet was infected with 5 mL of virus solution.

Experimental animal models

Three-day-old piglets were treated with oral antibiotics, in which gentamicin 3 mg, metronidazole 20 mg, and ampicillin 100 mg per kg of piglets were fed for 7 d. The CON group was fed for PBS 14 d as a control group, the ABX + LGG + PEDV group received PEDV infection after 7 d of antibiotic feeding and further LGG feeding, the ABX + PEDV group received PEDV infection after 7 d of antibiotic feeding and further PBS feeding.

q-PCR experiment

According to the manufacturer's instructions, total RNA was extracted, and 1 mg of RNA was reversed into cDNA by reverse transcriptase (Promega), which reverse transcribed the Moloney mouse leukemia virus. In the real-time quantitative PCR system of Applied Biosystems 7500, quantitative PCR was performed using SYBR Green mixture (TakBR Green). In the real-time quantitative PCR system of Applied Biosystems 7500, quantitative PCR was performed using SYBR Green mixture (Takara Bio). The average mRNA fold changes were calculated by $2^{-\Delta\Delta CT}$, and all primer sequences are shown in Supplementary Data 1.

Cell experiments

We stained the total LPL extracted from the lamina propria with antibodies

Live/Dead, CD45, Lin1 (CD3ε, CD21, γδ T, CD11c, CD172a), and Lin2 (CD4, CD8, CD163, CD11b) and then selected L/D-CD+Lin1-Lin2- cells by flow sorting or magnetic bead sorting (STEMCELL EasySep™ PE Positive Selection Kit). CD163, CD11b) and then selected L/D-CD45+Lin1-Lin2- cells by flow sorting or magnetic bead sorting (STEMCELL EasySep™ PE Positive Selection Kit II # 17684). After obtaining, they were cultured in vitro and then flow assayed. In order to maintain the cellular activity of ILCs, for all immunological cell cultures longer than 24h, we used OP9 cells co-cultured with immune cells to enhance the survival of ILC3 cells.

Organoid experiment

1. Piglets were euthanized by removing 8 cm of jejunum, removing the mesentery, dissecting the intestinal segments longitudinally, washing them with cold PBS until they were cleaned, cutting the segments into 0.5 cm pieces, washing them with cold PBS by blowing gently, and adding 15 mL PBS(2 mM EDTA). Let it stand at room temperature for 40 min.

2. Discard the supernatant, add 10 mL of DPBS, and blow 2 times. The supernatant was collected in a 50 mL centrifuge tube through a 70 μm cell sieve, labeled #1, and repeated 4 times. The filtrate of number 3 and 4 was centrifuged at 300 × g for 5 min, and the supernatant was discarded. The supernatant was resuspended with 1 mL of DME/F12(1% penicillin and streptomycin), transferred to a 1.5 mL centrifuge tube, centrifuged at 200 × g for 3 min, and the supernatant was discarded.

3. 250 μL of complete medium and 250 μL of Matrigel (operated on ice) were

244 added to the precipitate and blown to mix. Pipette 50 μL in the center of a 24-well
245 plate and place in the incubator for 30 min. Then, 500 μL medium (STEMCELL
246 #6000) was added to each well and 500 μL PBS to the remaining wells.
247 4. When the organoids start to germinate, they should be passaged. First, discard
248 the old medium and add 2 mL DME / F12, blow it up and down, and recycle it into
249 the centrifuge tube. After centrifugation, discard the supernatant and reintroduce it
250 into the complete medium and Matrigel.
251 **Isolation and Characterization of EVs**
252 EVs were isolated from *LGG* using ultracentrifugation. The size distribution and
253 morphology of EVs were analyzed by nanoparticle tracking analysis (NTA) and
254 transmission electron microscopy (TEM), respectively.
255 **Statistics**
256 Statistical analyses were performed using the statistical computer package, GraphPad
257 Prism version 6, (GraphPad Software Inc., San Diego, CA). Results are expressed as
258 means ± SEM. Statistical comparisons were made using two-way analysis of variance
259 with Tukey's post hoc test or Statistical comparisons were made using two-way
260 analysis of variance with Tukey's post hoc test or Student t test, where appropriate.
261 Differences were considered to be significant at $P < 0.05$. Significance is noted as $^{*}P < 0.05$, $^{**}P < 0.01$, $^{***}P < 0.001$ and $^{****}P < 0.0001$among groups
262
263
264 **Results**
265 **1. PEDV infection affects changes in the intestinal flora and ILC3 in piglets.**

In our previous work, we found a large number of immune cells in the piglet intestine (Wang et al., 2024), and through flow cytometric sorting and single-cell sequencing (scRNA-seq), we found that in Lin^- cells, there were a large number of ILCs cells (Fig. 1A), in which ILC3 expressing the signature transcription factor RORC was absolutely dominant (Fig. 1B), and also expressing, IL7R, AhR and other surface molecules, and secreted corresponding cytokines such as IL22 and IL17. The expression of these genes is important for the regulation and protection of intestinal homeostasis (Fig. 1C).

Through scRNA-seq analysis, we found that PEDV infection in piglets led to a significant decrease in the number of immune cells in the jejunum, including T cells and ILC3 (Fig. 1D, F, G). In contrast, non-immune cells, such as epithelial cells, exhibited abundant proliferation during the infection. (Fig. 1D, H). Despite the significant decrease in the number of ILC3 cells in the jejunum, the secretion of IL-22 was markedly increased (Fig. 1E, I). These results suggest that the increased secretion of IL-22 by ILC3 cells may play a crucial role in conferring resistance against PEDV during PEDV infection. Our flow cytometry assay results were consistent with the single-cell results, the flow gating strategy in Fig. S1A. These results also confirmed a significant decrease in the number of ILC3 cells in the intestinal lamina propria of PEDV-infected piglets, accompanied by an up-regulation of IL-22 secretion by ILC3 cells (Fig. 1J). Furthermore, our findings revealed significant alterations in the flora of the jejunum in PEDV-infected piglets. At both the order level and the genus level, there was a notable decrease in the levels of *Lactobacillales* orders and *Lactobacillus*

genus (Fig. 1K, L).

To further investigate the underlying cause of the significant changes in ILC3 during PEDV infection, we aimed to discern whether these changes were primarily driven by viral infection or influenced by alterations in the bacterial flora. To explore this, we conducted an experiment involving antibiotic treatment to manipulate the structure of the flora. By observing the effects of this flora change on the body's immunity, we aimed to gain insights into the intricate relationship between the microbial composition and the immune response.

2. Alteration of intestinal flora may affect ILC3 development.

In our study, we initially established a dysregulation model of piglets' microflora. We observed significant impacts on the immune development of piglets with dysflora. Specifically, there was a noticeable reduction in the number of CD4-T cells in the jejunum lamina propria (Fig. S2A). Additionally, the development of ILC3 was even more severely affected, with a significant decrease in cell numbers and an increase in IL-22 secretion (Fig. 2A). Meanwhile, antibiotic treatment resulted in the decrease of flora richness and *lactobacillus* number in the jejunum of piglets (Fig. 2B, C). Linear discriminant analysis Effect Size (LEfSe) analysis identified significantly different taxa between groups, which were significantly enriched from the point of view of order, genus, and species, respectively, belonging to *Lactobacillales*, *Lactobacillaceae*, and *Lactobacillus* (Fig. 2D, E, F, G).

The above results suggest that the number of immune cells, especially ILC3, was significantly affected under both PEDV infection and antibiotic treatment conditions

and that this change persisted when only the flora was changed. The flora may play a very important role in the interactions with ILC3, and if there is a regulatory effect of the flora on ILC3, by what pathway does the flora regulate ILC3? Up-regulation of indole analogs, including bisindolylmaleimide I and indoxyl sulfate, has been reported in PEDV infection (Li et al., 2022). Non-targeted metabolomics was further analyzed for the metabolites in jejunum samples. As a result, we found significant changes in some AhR-related regulatory substances in both positive and negative ion modes (Fig. 2H, I, J, K), especially many indoles that have been repeatedly shown to have a significant activating effect on the AhR. We further performed enrichment analyses and found a significant enrichment in important immune-regulatory pathways such as tryptophan. To investigate whether differential microbial communities produce differential metabolites, we conducted a combined analysis of 16S and metabolomics. The results revealed a significant decrease in the abundance of regulatory substances secreted by probiotic bacteria, leading to a reduction in their overall levels. However, unfortunately, we did not directly associate the metabolites with the production by *Lactobacillus* (Figure S2B, C).

So far, the expression of the AhR receptor has been studied in immune cells in humans and mice, but its expression has not been reported in pigs. Furthermore, the expression of AhR in immune cells in the intestine is unknown. We found that immune cells in the porcine intestine highly expressed AhR receptors by single-cell analysis (Fig. 2L), and further analysis revealed that ILC3 in the intestine expressed high levels of AhR (Fig. 2M). In human intestinal ILC, both ILC3 and ILC1 highly

expressed AhR receptors (Fig. S2D), whereas only ILC2 expressed AhR in the murine upper intestine (Fig. S2E). These results suggest that porcine and human intestinal ILC3 exhibit high levels of AhR activation, indicating that ILC3 in the intestine may respond significantly to stimulation by AhR ligand-related substances.

3. Feeding *LGG* can enhance the piglets' immunity against PEDV infection.

To explore whether *Lactobacillus* can resist PEDV infection in the gut, we selected the standard *Lactobacillus* strain *LGG* to supplement piglets with an intestinal flora imbalance and then carried out a PEDV challenge experiment. Our objective was to determine whether feeding *LGG* could enhance intestinal immunity, specifically by activating ILC3 cells, thereby promoting intestinal homeostasis and conferring resistance against PEDV infection.

It was found that *LGG* supplementation significantly reduced the pathological changes of PEDV infection in piglets, and the intestinal tract was healthy in the CON group. The villi of the jejunum of piglets in the ABX+*LGG*+PEDV group were shortened and atrophied, and the epithelial cells were mildly diseased. The villi of the jejunum in piglets from the ABX+PEDV group exhibited shortened, fragmented, and broken structures. Additionally, the intestinal epithelial cells underwent typical histopathological changes such as vacuolization, fusion lesions, necrosis, and detachment following PEDV infection (Fig. 3A). The ratio of villus height to crypt depth (VH/CD) of the jejunum villi of piglets in each infection group was found to be significantly lower in the ABX+PEDV group than in the ABX+*LGG*+PEDV group (Fig. 3B). The diarrhea scoring results proved that feeding *LGG* alleviated diarrhea in

354 piglets (Fig. 3C). Next, we found significant differences in viral loads in the
355 duodenum, jejunum and ileum between the ABX+*LGG*+PEDV group and the
356 ABX+PEDV group, especially in the jejunum and ileum, where the viral copy number
357 was significantly decreased after feeding *LGG* (Fig. 3E).

358 Flow results also demonstrated a significant increase in the amount of ILC3 in
359 the intestines of the ABX+*LGG*+PEDV group, which was close to that of the CON
360 group and significantly higher than that of the ABX+PEDV group. The secretion of
361 IL-22 was also significantly lower than that of the ABX+PEDV group, suggesting that
362 the inflammatory state of the jejunum intestinal tract of the piglets was ameliorated in
363 response to the infection (Fig. 3D). A dramatic improvement also occurred in the
364 abnormal activation state of the intestinal tract through stimulation by feeding *LGG* to
365 promote proliferation of epithelial cells and the production of IL-22 after viral
366 infection, including the expression of proteins such as EpCAM and VILLIN in the
367 intestinal tract (Fig. 3F). There was also a significant reduction in the cell
368 proliferation-related proteins LGR5 and Ki-67 (Fig. S3A).

369 Our results at the mRNA level were consistent with the results at the protein
370 level, revealing that inflammation-related genes such as IL-22 and IL-1β, the
371 epithelial gene EpCAM, the villi gene VILLIN, the proliferation and
372 differentiation-related gene MKI-67, the ISC labeling genes Lgr5, Ascl2, Olfm4, and
373 the Paneth cell activation genes Lyz1 and REG3b were all significantly reduced
374 (Figure S3B). Feeding *LGG* also significantly increased the abundance of intestinal
375 flora in piglets, particularly the number of the *Lactobacillus* genus, and elevated the

content of other probiotics, such as *Streptococcus spp*, suggesting that feeding *LGG* can promote the recovery of the intestinal flora (Fig. S3C).

4. *In vitro* cellular experiments demonstrated that *LGG* metabolites promote ILC3 cell activation to resist PEDV.

We first successfully constructed an in vitro culture model of ILC3 (Fig. S4A), performed a flow cytometry assay under different stimulant-inducing conditions, and developed a gating strategy (Fig. S4B). We found that both *LGG*-secreted extracellular vesicles (EVs) and Indole-3-carbinol (I3C) could significantly promote ILC3 proliferation and secretion of IL-22 through activation of the AhR. The effect disappeared when the AhR antagonist CH-223191 (CH) was added (Fig. 4A).

Previous correlational studies have indicated the possibility of ILC transformation within the organism, particularly when induced by specific conditions (Bal et al., 2020). To investigate whether the change in the number of ILC3 is due to the transformation of other immune cells, we conducted magnetic bead sorting on ILCs cells and subsequently examined them using SFSE staining(Fig. S4C). We discovered that ILC3 is the primary cell population within ILCs where proliferation occurs. The proliferation of ILCs cells dominated by ILC3 was significantly stronger than that of other non-ILC cells (Fig. S4D). The expression of ILC3-related cytokines, including IL-22, IL-17A, IL-17B, CXCL2, and CXCL8, were all found to be significantly up-regulated (Fig. 4B).

Our study investigated whether the activation of ILC3 and secretion of IL-22 promoted by EVs are effective in enhancing the resistance of porcine epithelial cells

to PEDV infection. We established a co-culture model of ILC3 and IPEC-J2 cells (Fig. S4E) and observed that IL-22 secreted by EVs-promoted ILC3 had a positive impact on IPEC-J2 cell proliferation and the activation of STAT3 (Fig. 4C). Furthermore, when EVs and ILC3 were added to co-cultured IPEC-J2 cells after PEDV infection, it significantly influenced the outcome of PEDV infection by preventing apoptosis of IPEC-J2 cells (Fig. 4D), the gating strategy in Fig. S4F.

These results suggest that EVs derived from *LGG* can stimulate the proliferation and secretion of IL-22 by ILC3 through the AhR receptor on ILC3. This process promotes the proliferation and activation of epithelial cells and enhances the expression of the STAT3 gene. Therefore, it alleviates IPEC-J2 apoptosis caused by PEDV infection.

5. Porcine intestinal organoid proving experiments.

We successfully constructed an in vitro model of organoids from the jejunum of piglets. The size of isolated intestinal crypts was about 15 μm, and they were cultured with matrigel. The first generation of organoids grew slowly and developed into mature bodies with a diameter of about 200 μm by the eighth day and were continued to be cultured. Then they died and fragmented, and displayed a large number of buds in 5-8 d and could be propagated through passaging culture(Fig. 5A). Subsequently, the cultured organoids grew rapidly after passaging, reaching a size of 100 μm in three d and matured into bodies with a diameter of 200 μm within 5 d (Figure S5B).

Previous experiments have shown that EVs can stimulate the secretion of IL-22 from ILC3. Therefore, it is worth investigating if IL-22, secreted by ILC3, can

promote the growth of organoids. In our study, we initially supplemented the intestinal organoid medium with HK *LGG* and EVs derived from *LGG* (Fig. 5B). We then monitored the number of organoids, organoid size, and germination rate throughout the organoid growth process. Interestingly, we observed that the addition of HK *LGG* and EVs alone did not have any noticeable effect on the development of organoids (Fig. 5D).

In the next phase of our study, we successfully established a co-culture system involving intestinal organoids, stimulatory molecules, and ILC3 cells (Fig. 5C). Initially, we attempted to culture ILC3 cells by adding them directly to the matrigel. However, this method proved unsuitable for the survival of ILC3 cells and resulted in severe cell death and fragmentation within 24 h. To overcome this issue, we performed co-cultures using a transwell system with a pore size of 0.4 μm. We renewed the upper layer of ILC3 cells every 24 h. Notably, we observed that the growth of the organoids was significantly enhanced in the co-culture system when EVs+ILC3 and IL-22 were added. Within the first two d, the organoids experienced rapid growth, reaching a size of 70 μm. Subsequently, they started to exhibit significant budding and divided into multiple crypts on the third day. The organoids continued to grow rapidly, whereas the promotional effect of EVs and IL-22 on organoid growth disappeared upon the addition of an antibody specific to IL-22. Importantly, the number of organoids was not affected (Fig. 5E). Comparing the experimental group (EVs+ILC3, IL-22) with the control group (including ILC3, ILC3+EVs(*LGG*)+anti-IL-22, IL-22+anti-IL-22), we found that the experimental

group significantly promoted the growth of the organoids. Notably, a significant difference was observed on the third day during germination, and by the sixth day, the size of the organoids in the experimental group showed significant differences compared to the control (Fig. 5F).

Next, immunofluorescence results revealed significant expression of proliferation-related proteins in organoids after addition of co-cultures of EVs+ILC3 and IL-22, including increased expression of 5-Ethynyl-2′-deoxyuridine (EdU) (Fig. 5G), the ISCs activation-related protein LGR5, and the cell proliferation-related protein Ki67; a significant increase in expression of the epithelial Significantly increased expression of the epithelial protein EpCAM and the chorionic protein VILLIN was also found (Fig. S5C). Q-PCR results also identified the epithelial gene EpCAM, the chorionic gene VILLIN, the proliferation and differentiation-associated gene MKI-67, and the ISCs marker genes Lgr5, Ascl2, and Olfm4 in the class of organoids following the incorporation of co-cultures of EVs+ILC3 and IL-22; and Paneth cell activation genes Lyz1 and REG3b were significantly increased (Fig. 5H).

These results demonstrated that the EVs of LGG could significantly promote the growth and development of organoids and activate ISCs, Paneth cells, epithelial cells, and other cells in organoids.

6. The metabolites of *LGG* are rich in AhR ligands, such as indole compounds.

We further examined the *LGG*-produced EVs and found the diameter of the EVs to be around 70 nm by nanoflow cytometry (Fig. 6A). The signature horseshoe-shaped structure of the EVs, which contained a large amount of *LGG*

464 metabolites, was visualized under an electron microscope (Fig. 6B).

465 We enriched and collected the extracellular vesicles (EVs) through ultrafast
466 centrifugation. Subsequently, we conducted off-target metabolism detection. In total,
467 414 substances were identified in the positive mode (POS), while 326 substances
468 were detected in the negative mode (NEG). We observed a significant presence of
469 lipids and lipid-like molecules, as well as organic acids and derivatives, in both the
470 POS and NEG modes (Fig. 6C). We found a wide range of substances that can interact
471 with AhR, including indole compounds such as L-5-Hydroxytryptophan and
472 Indole-3-acrylic acid, as well as several ketone compounds, and some ketones.
473 Research has indicated that, apart from indoles, ketones can also interact with AhR
474 (Amakura et al., 2008).

475 We conducted KEGG enrichment analysis on the total metabolites and found
476 significant enrichment in the Metabolism pathway. Additionally, enrichment was
477 observed in pathways such as Cellular Processes, Environmental Information
478 Processing, and Genetic Information Processing (Fig. 6D).

479 Our study provides insights into the interaction between ILC3s in the porcine
480 small intestine and *Lactobacillus*, aiming to understand better how they interact. We
481 have demonstrated that oral *LGG* is a potential approach for preventing PEDV
482 infection in pigs. It can alleviate intestinal inflammation, intestinal damage, and
483 clinical diarrhea symptoms caused by PEDV infection. We found that EVs (*LGG*) can
484 activate ILC3s and promote IL-22 secretion, thereby influencing intestinal stem cell
485 regeneration and epithelial protection. Ultimately, this helps to purify the gut

environment and resist PEDV infection. In summary, our research demonstrates that oral *LGG* promises to be a potential method for preventing PEDV infection in pigs. Furthermore, it opens up new avenues for preventing PEDV infection in piglets.

Discussion

Recently, we discovered the presence of ILCs in the jejunum of piglets. These cells are predominantly ILC3 and play a crucial role in maintaining intestinal immune homeostasis. In our study, we further elucidated the interaction between ILC3 and the gut microbiota, particularly *Lactobacillus*, in the jejunum of piglets to maintain intestinal homeostasis. Based on our findings and existing literature, we constructed a pathway diagram illustrating how EVs produced by *LGG* facilitate the secretion of IL-22 by ILC3 cells. IL-22, in turn, acts on downstream targets such as epithelial cells, Paneth cells, and ISCs to regulate intestinal immune function, thereby conferring protection against PEDV infection (Figure 6E).

The gut microbiota plays a crucial role in the development and maintenance of the host immune system, and its complexity is undeniable. It stabilizes mucosal function by maintaining the integrity of the gut barrier and balances the inflammatory response with immune tolerance through the induction of T lymphocyte differentiation. Additionally, the gut microbiota promotes the development of early B lymphocytes in the lamina propria of the mouse small intestine (Zegarra-Ruiz et al., 2021; Rooks and Garrett, 2016). At the same time, the immune system also regulates the microbial community in a certain way to maintain relative balance. However,

508 changes in this balance are often associated with the occurrence or progression of
509 diseases. Probiotics have a positive effect on the gut microbiota, especially in the
510 innate and adaptive immune systems. Preclinical studies and clinical practice have
511 shown that the use of probiotics can limit the overgrowth of pathogenic bacteria and
512 control the host's pathological processes (Pitocco et al., 2020). Furthermore, the
513 interaction between bacteria and host cells is a complex process that has yet to be
514 fully understood and deserves further exploration. Our research revealed significant
515 changes in the gut microbiota during PEDV infection, including a decrease in the
516 abundance of beneficial bacteria such as *Lactobacillus*. However, oral administration
517 of *LGG* can greatly alleviate dysbiosis and increase the diversity of the gut
518 microbiota.

519 AhR is a widely expressed transcription factor in immune system cells,
520 particularly playing a crucial role in intestinal immune cells. Studies have shown that
521 AhR activation specifically alters innate and adaptive immune responses and
522 participates in the regulation of cell differentiation and inflammation-related gene
523 expression. Furthermore, inducible AhR activation may serve as a mechanism by
524 which the gut microbiota promotes mucosal homeostasis. In comparison to its role in
525 intestinal immune cells, the function of AhR in intestinal epithelial cells (IECs) has
526 not been extensively studied. Previous research has found a close association between
527 AhR in IECs and the maintenance of epithelial barrier function (Qian et al., 2022).
528 One of the endogenous ligands for AhR is a metabolite of tryptophan. The gut
529 microbiota can convert tryptophan into various molecules, including ligands for AhR,

530 such as indole and its derivatives (e.g., IAld, IAA, IPA, IAAld, and indole-3-acrylic
531 acid). The AhR signaling pathway is an essential component for maintaining barrier
532 immune responses, promoting epithelial cell recovery, preserving barrier integrity, and
533 regulating certain immune cell functions to maintain gut homeostasis. The gut
534 microbiota and tryptophan and its metabolites interact closely in various aspects,
535 including gut barrier function, gut immunity and endocrine activity, and intestinal
536 motility (Su et al., 2022). Current research has described a few commensal bacteria,
537 such as *Lactobacillus*, capable of producing AhR ligands (Agus et al., 2018).
538 However, the significance of these complex phenomena in the intestinal system still
539 requires further investigation. One study discovered that adaptive lactobacilli can
540 expand and produce an AhR ligand, I3A, which contributes to the transcription of
541 IL-22 dependent on AhR. Therefore, the microbiota-AhR axis may serve as an
542 important strategy for modulating host mucosal immune responses in symbiotic
543 evolution (Zelante et al., 2013).

544 Additionally, lactobacilli can regulate immune cells through AhR by producing
545 substances like tryptophan and expressing tryptophanase, thus promoting the
546 production of indole-3-propionic acid associated with human health (Liu et al., 2023).
547 Our research findings demonstrate that in a healthy state of piglet gut microbiota,
548 there is a higher proportion of *Lactobacillus*. Additionally, we observed a significant
549 presence of substances in the gut that interact with AhR. Moreover, AhR exhibits
550 notable upregulation of porcine immune cells, particularly ILC3, indicating a
551 potentially tighter regulatory relationship between ILC3 and the gut microbiota via

552 AhR in the pig gut. In states of PEDV infection or dysbiosis, the levels of substances
553 interacting with AhR significantly increase in the gut. Activation of ILC3 and
554 secretion of IL-22 are subsequently promoted through AhR, thereby exacerbating
555 inflammation and accelerating stimulation and activation of downstream receptor
556 cells by IL-22. However, oral administration of *LGG* to piglets leads to significant
557 restoration of gut microbiota balance and the regulatory relationship between
558 metabolites and AhR.

559 IL-22 is a member of the IL-10 family that can be produced by ILCs and CD4-T
560 cells. The IL-22-IL-22R signaling axis plays a crucial role in integrating immune
561 responses with mucosal surface barrier function (Makowski et al., 2020; Dudakov et
562 al., 2015). Increasing evidence suggests that IL-22 plays an important role in
563 inflammatory bowel disease (IBD) (Mizoguchi 2012). IL-22 produced by ILC3 is
564 essential for maintaining intestinal homeostasis and provides early protection to
565 epithelial barrier function during inflammation and injury (Zenewicz et al., 2008). The
566 interaction between the microbiota and IL-22 is central to regulating the barrier sites
567 in intestinal homeostasis. On the one hand, IL-22 promotes intestinal barrier function
568 by inducing antimicrobial peptides, mucins, and other beneficial factors from
569 epithelial cells, thereby modulating the composition of the gut microbiota. On the
570 other hand, the gut microbiota also regulates the production of intestinal IL-22,
571 although the underlying mechanisms are not fully understood. Research has reported
572 that many functions of the gut microbiota in regulating health and disease are
573 mediated through their metabolites (Lynch and Pedersen 2016, Rooks and Garrett

574 2016). In our in vitro experiments using IPEC-J2 cells and piglet intestinal organoids,
575 we found that EVs produced by *LGG* can promote the activation of ILC3 cells and the
576 production of IL-22. The generated IL-22 can act on IPEC-J2 cells, promoting their
577 proliferation, activating the STAT3 signaling pathway, and conferring resistance
578 against PEDV infection. Moreover, the produced IL-22 can also act on Paneth cells,
579 ISCs, and epithelial cells within the organoids to promote their growth and
580 development.

581 Investigators have found that IFN-γ and IL-22 act synergistically to induce
582 interferon-stimulated genes and control rotavirus infection. Therefore, this pathway
583 may not be specific to PEDV infection and could potentially play a role in other
584 diseases as well (Hernández et al., 2015). Although we observed significant changes
585 in the secretion of ILC3 and IL-22 in the jejunum of piglets following exposure to
586 *Lactobacillus*, it is still unknown whether other bacteria can significantly stimulate
587 ILC3 to secrete IL-22. Could it be possible that the balance between lactobacilli and
588 ILC3 is disrupted, leading to dysregulation of the existing regulatory relationship and
589 a significant increase in the number of harmful bacteria, thereby further stimulating
590 ILC3 activation? These questions remain unanswered, and we hope to address them in
591 future research.

592 Currently, there is increasing interest in studying the interactions between
593 microorganisms and the immune system. On the one hand, the immune system can
594 regulate and shape the microbial community, and on the other hand, the established
595 microbial community can promote the development of the host's immune system and

provide signals for subsequent immune responses. However, our understanding of the interactions between microorganisms and the immune system is still limited, and unraveling these complexities requires interdisciplinary collaboration and innovation. Numerous intrinsic factors influence the balance within the animal body. Although our research focuses on the interaction between intestinal lactobacilli and ILC3 through the AhR, it is important to note that there are countless regulatory pathways within the animal body. Moreover, research on pigs is relatively scarce, and much of our knowledge comes from studies conducted on humans and mice. Therefore, we cannot fully comprehend the complete role of ILC cells in the intestinal immunity of pigs. Furthermore, considering that ILC3 is an emerging cell type in pigs, our work is just the beginning. In the future, we will explore the changes in this cell population during intestinal immunity and disease states, laying the foundation for studying intestinal immunity in pigs.

Acknowledgments

We thank Dr. Guangliang Liu Provided to us with the PEDV strain. We thank Dr. Xuechao Gao from Geneu Biotech Co., Ltd., who helped us obtain monoclonal antibodies against porcine IL-22. We thank Novogene Co., for providing technical services such as detecting and analyzing of scRNA-seq raw data, 16S rDNA sequencing and Metabolome sequencing.

Data availability statement

The raw data for this article were deposited in the National Center for Biotechnology Information (NCBI) Sequence Read Archive (SRA) database, Gene Expression Omnibus (GEO) database and EBI database. The source of the jejunal single cell data after PEDV infection in piglets is GSE175411. Single cell data of piglet jejunum ILCs in PRJNA907920. We comparisons with Human intestinal ILCs (GSA-Human: HRA000919) and mouse intestinal ILCs (GSE166266). 16S rRNA amplicon sequencing data in PRJNA526581, PRJNA1048561 and PRJNA1048648.

Author contributions

Cell isolation, J.H.W., Y.B.Z., and T.C.; data analysis, J.H.W., H.Y.B., M.G., Y.S., and Y.Y.L.; manuscript preparation and writing, J.H.W., Y.Y.L., M.Y.C., and H.Y.B.; Information collection, Y.B.Z., T.C., and H.Y.B.; supervision and project administration, C.F.W., Y.Z., and X.C. Preparation of experimental reagent materials, C.W.S., J.Y.G., J.Z.W., N.W., W.T.Y., Y.L.J., H.B.H., D.Z., J.T.H., G.L.Y. All authors contributed to the article and approved the submitted version.

Ethics declarations

Consent to publish

All authors have approved the content of this manuscript and provided consent for publication.

Conflict of Interest

The authors declare that the research was conducted without any commercial or financial relationships that could be construed as a potential conflict of interest.

Ethics

The animal management procedures and all laboratory procedures abided by the regulations of the Animal Care and Ethics Committees of Jilin Agriculture University, China.

Funding

This work was supported by the National Natural Science Foundation of China (32273043, 32202890, U21A20261), the Science and Technology Development Program of Changchun City (21ZY42), the Science and Technology Development Program of Jilin Province(20200402041NC), and China Agriculture Research System of MOF and MARA (CARS-35).

This paper does not report the original code. Any additional information required to reanalyze the data reported in this paper is available from the lead contact upon request.

660 **References**

661 Agus A, Planchais J, Sokol H (2018). Gut Microbiota Regulation of Tryptophan
662 Metabolism in Health and Disease. *Cell host & microbe* 23: 716-724.

663

664 Amakura Y, Tsutsumi T, Sasaki K, Nakamura M, Yoshida T, Maitani T (2008).
665 Influence of food polyphenols on aryl hydrocarbon receptor-signaling pathway
666 estimated by in vitro bioassay. *Phytochemistry* 69: 3117-3130.

667

668 Aparicio-Domingo P, Romera-Hernandez M, Karrich J, Cornelissen F, Papazian N,
669 Lindenbergh-Kortleve D et al (2015). Type 3 innate lymphoid cells maintain intestinal
670 epithelial stem cells after tissue damage. *The Journal of experimental medicine* 212:
671 1783-1791.

672

673 Backert I, Koralov S, Wirtz S, Kitowski V, Billmeier U, Martini E et al (2014). STAT3
674 activation in Th17 and Th22 cells controls IL-22-mediated epithelial host defense
675 during infectious colitis. *Journal of immunology* (Baltimore, Md : 1950) 193:
676 3779-3791.

677

678 Bal S, Golebski K, Spits H (2020). Plasticity of innate lymphoid cell subsets. *Nature*
679 *reviews Immunology* 20: 552-565.

680

681 Chen J, Cui Y, Wang Z, Liu G (2020). Identification and characterization of PEDV

682 infection in rat crypt epithelial cells. *Veterinary microbiology* 249: 108848.

683

684 Dudakov J, Hanash A, van den Brink M (2015). Interleukin-22: immunobiology and
685 pathology. *Annual review of immunology* 33: 747-785.

686

687 Gury-BenAri M, Thaiss C, Serafini N, Winter D, Giladi A, Lara-Astiaso D et al
688 (2016). The Spectrum and Regulatory Landscape of Intestinal Innate Lymphoid Cells
689 Are Shaped by the Microbiome. *Cell* 166: 1231-1246.e1213.

690

691 Hanash A, Dudakov J, Hua G, O'Connor M, Young L, Singer N et al (2012).
692 Interleukin-22 protects intestinal stem cells from immune-mediated tissue damage and
693 regulates sensitivity to graft versus host disease. *Immunity* 37: 339-350.

694

695 Hernández P, Mahlakoiv T, Yang I, Schwierzeck V, Nguyen N, Guendel F et al (2015).
696 Interferon-λ and interleukin 22 act synergistically for the induction of
697 interferon-stimulated genes and control of rotavirus infection. *Nature immunology* 16:
698 698-707.

699

700 Jung K, Saif L (2015). Porcine epidemic diarrhea virus infection: Etiology,
701 epidemiology, pathogenesis and immunoprophylaxis. *Veterinary journal* (London,
702 England : 1997) 204: 134-143.

703

704 Kiss E, Vonarbourg C, Kopfmann S, Hobeika E, Finke D, Esser C et al (2011).
705 Natural aryl hydrocarbon receptor ligands control organogenesis of intestinal
706 lymphoid follicles. *Science* (New York, NY) 334: 1561-1565.
707
708 Li Z, Zhang W, Su L, Huang Z, Zhang W, Ma L et al (2022). Difference analysis of
709 intestinal microbiota and metabolites in piglets of different breeds exposed to porcine
710 epidemic diarrhea virus infection. *Frontiers in microbiology* 13: 990642.
711
712 Lindemans C, Calafiore M, Mertelsmann A, O'Connor M, Dudakov J, Jenq R et al
713 (2015). Interleukin-22 promotes intestinal-stem-cell-mediated epithelial regeneration.
714 *Nature* 528: 560-564.
715
716 Liu L, Narrowe A, Firrman J, Mahalak K, Bobokalonov J, Lemons J et al (2023).
717 Lacticaseibacillus rhamnosus Strain GG (LGG) Regulate Gut Microbial Metabolites,
718 an In Vitro Study Using Three Mature Human Gut Microbial Cultures in a Simulator
719 of Human Intestinal Microbial Ecosystem (SHIME). *Foods* (Basel, Switzerland) 12.
720
721 Lynch S, Pedersen O (2016). The Human Intestinal Microbiome in Health and
722 Disease. *The New England journal of medicine* 375: 2369-2379.
723
724 Makowski L, Chaib M, Rathmell J (2020). Immunometabolism: From basic
725 mechanisms to translation. *Immunological reviews* 295: 5-14.

Mizoguchi A (2012). Healing of intestinal inflammation by IL-22. *Inflammatory bowel diseases* 18: 1777-1784.

Pernomian L, Duarte-Silva M, de Barros Cardoso C (2020). The Aryl Hydrocarbon Receptor (AHR) as a Potential Target for the Control of Intestinal Inflammation: Insights from an Immune and Bacteria Sensor Receptor. *Clinical reviews in allergy & immunology* 59: 382-390.

Pitocco D, Di Leo M, Tartaglione L, De Leva F, Petruzziello C, Saviano A et al (2020). The role of gut microbiota in mediating obesity and diabetes mellitus. *European review for medical and pharmacological sciences* 24: 1548-1562.

Qian M, Liu J, Zhao D, Cai P, Pan C, Jia W et al (2022). Aryl Hydrocarbon Receptor Deficiency in Intestinal Epithelial Cells Aggravates Alcohol-Related Liver Disease. *Cellular and molecular gastroenterology and hepatology* 13: 233-256.

Ronan V, Yeasin R, Claud E (2021). Childhood Development and the Microbiome-The Intestinal Microbiota in Maintenance of Health and Development of Disease During Childhood Development. *Gastroenterology* 160: 495-506.

Rooks M, Garrett W (2016). Gut microbiota, metabolites and host immunity. *Nature*

reviews Immunology 16: 341-352.

Satoh-Takayama N, Vosshenrich C, Lesjean-Pottier S, Sawa S, Lochner M, Rattis F et al (2008). Microbial flora drives interleukin 22 production in intestinal NKp46+ cells that provide innate mucosal immune defense. *Immunity* 29: 958-970.

Su X, Gao Y, Yang R (2022). Gut Microbiota-Derived Tryptophan Metabolites Maintain Gut and Systemic Homeostasis. *Cells* 11.

Wang J, Gao M, Cheng M, Luo J, Lu M, Xing X et al (2024). Single-Cell Transcriptional Analysis of Lamina Propria Lymphocytes in the Jejunum Reveals Innate Lymphoid Cell-like Cells in Pigs. *Journal of immunology* (Baltimore, Md : 1950).

Xia P, Liu J, Wang S, Ye B, Du Y, Xiong Z et al (2017). WASH maintains NKp46 ILC3 cells by promoting AHR expression. *Nature communications* 8: 15685.

Xue M, Zhao J, Ying L, Fu F, Li L, Ma Y et al (2017). IL-22 suppresses the infection of porcine enteric coronaviruses and rotavirus by activating STAT3 signal pathway. *Antiviral research* 142: 68-75.

Yan F, Liu L, Cao H, Moore D, Washington M, Wang B et al (2017). Neonatal

colonization of mice with LGG promotes intestinal development and decreases susceptibility to colitis in adulthood. *Mucosal immunology* 10: 117-127.

Yang S, Li Y, Wang B, Yang N, Huang X, Chen Q et al (2020a). Acute porcine epidemic diarrhea virus infection reshapes the intestinal microbiota. *Virology* 548: 200-212.

Yang S, Li S, Lu Y, Jansen C, Savelkoul H, Liu G (2023). Oral administration of Lactic acid bacteria inhibits PEDV infection in young piglets. *Virology* 579: 1-8.

Yang W, Yu T, Huang X, Bilotta A, Xu L, Lu Y et al (2020b). Intestinal microbiota-derived short-chain fatty acids regulation of immune cell IL-22 production and gut immunity. *Nature communications* 11: 4457.

Yu L, Agirman G, Hsiao E (2022). The Gut Microbiome as a Regulator of the Neuroimmune Landscape. *Annual review of immunology* 40: 143-167.

Zegarra-Ruiz D, Kim D, Norwood K, Kim M, Wu W, Saldana-Morales F et al (2021). Thymic development of gut-microbiota-specific T cells. *Nature* 594: 413-417.

Zelante T, Iannitti R, Cunha C, De Luca A, Giovannini G, Pieraccini G et al (2013). Tryptophan catabolites from microbiota engage aryl hydrocarbon receptor and

792 balance mucosal reactivity via interleukin-22. *Immunity* 39: 372-385.

793

794 Zenewicz L, Yancopoulos G, Valenzuela D, Murphy A, Stevens S, Flavell R (2008).

795 Innate and adaptive interleukin-22 protects mice from inflammatory bowel disease.

796 *Immunity* 29: 947-957.

797

798

799

800

801

802

803

804

805

806

807

808

809

810

811

812

813

Figure legends

Fig. 1 | PEDV infection resulted in abnormal changes in both the intestinal flora and ILC of piglets.

A: UMAP plots showing the immune landscape of the 12 subpopulations of the intestine cell(Selection by flow cytometry). B: UMAP plots showing the immune landscape of the 4 clusters of intestine cells (ILC regrouping). Cells are color-coded according to the defined subset (ILC3: yellow; ILC1: red; ILC2: green; NK: blue). C: Heatmap showing the marker genes with some highest differentially expressed in each cluster, Abscissa shows different clusters, and ordinate shows differentially expressed gene names. D: UMAP plots showing the immune landscape of intestine cells in the jejunum of piglets in both PEDV-infected and normal states. E: The amount of ILC3 significantly decreased, while the secretion of IL-22 was significantly increased. F: Variations in the quantity of immune cells. G: Variations in the quantity of ILC3. H: Variations in the quantity of epithelial cells. I: Differential changes in the secretion of IL-22 by ILC3. J: The amount of ILC3 in the intestinal lamina propria of PEDV-infected piglets significantly decreased, and the secretion of IL-22 increased. K: Changes in Lactobacillales orders in the intestinal tract of piglets. J: Changes in Lactobacillus Genus in the intestinal tract of piglets.

Fig. 2 | The imbalance of intestinal flora may affect the development of ILC3.

A: The number of ILC3 in the intestinal lamina propria of piglets with intestinal flora disturbance decreased significantly, and the secretion of IL-22 increased. B: The Venn

836 diagram showed the difference of intestinal flora species between the PBS and ABX
837 groups (α Diversity). C: PCA analysis between the PBS and ABX groups (β
838 Diversity). D: LDA Effect Size (LEfSe) analysis between the PBS and ABX groups (β
839 Diversity). E: Changes in Lactobacillales orders in the intestinal tract of piglets. F:
840 Changes in Lactobacillaceae family in the intestinal tract of piglets. G: Changes in
841 Lactobacillus genus in the intestinal tract of piglets. H: Changes in differential
842 metabolites in the negative ion mode. I: Changes in differential metabolites in the
843 positive ion mode. J: Different substances were observed between the groups in
844 negative ion mode, with a particular focus on substances that are associated with AHR.
845 K: Different substances were observed between the groups in negative ion mode, with
846 a particular focus on substances that are associated with AHR. L: UMAP and violin
847 plots showing the AHR was prominently expressed in immune cells within pig
848 intestines. M: UMAP and violin plots showing the AHR was prominently expressed in
849 ILC3 within pig intestines.
850
851 Fig. 3 | LGG can help piglets resist PEDV infection
852 A: Feeding LGG can significantly alleviate the pathological changes of jejunum in
853 piglets. B: The ratio of villus height to crypt depth (VH/CD) of intestinal villi of
854 piglets. C: Piglet diarrhea score. 0= normal stool, 1= soft but formed stool, 2=
855 semi-liquid stool, 3= watery diarrhea, with a score of 2 or more considered diarrhea.
856 D: Flow cytometry showed the change of ILC3 quantity and IL-22 secretion in the
857 intestinal tract of piglets. E. The q-PCR results showing viral load in the intestines of

858 piglets. F: Immunofluorescence assay showed the expression of EpCAM and VILLIN
859 in the gut, Analysis by image J software.
860
861 Fig. 4 | Experimental results of LGG metabolites promoting ILC3 cell activation
862 A: Flow cytometry showed that I3C and EVs can promote the amount of ILC3 and
863 the secretion of IL-22 under co-culture conditions. B: Transcriptional levels of
864 ILC3-related cytokines stimulated by LGG metabolites were measured by q-PCR. C:
865 Statistics of the number of IPEC-J2 cells; The transcription level of STAT3 gene in
866 IPEC-J2 cell species was detected by q-PCR. D: Flow cytometry calculates the
867 percentage of cells that die. The Annexin V-/PI+ cells in the upper left quadrant may
868 represent cell fragments lacking cell membranes or dead cells resulting from other
869 causes. The Annexin V-/PI- cells in the lower left quadrant are considered normal and
870 alive. The Annexin V+/PI+ cells in the upper right quadrant are indicative of late
871 apoptotic cells. Lastly, the Annexin V+/PI- cells in the lower right quadrant also
872 correspond to early apoptotic cells.
873
874 Fig. 5 | Piglet intestinal organoids experiment
875 A: Crypts isolated from piglet intestines were cultured in vitro, and the images depict
876 the changes in organoid size over an eight-day period. B: HK LGG and EVs were
877 added to the intestinal organoid culture hole. C: The co-culture system consisted of
878 intestinal organoids, along with associated stimulatory molecules and ILC3 cells. D:
879 Effects of HK LGG and EVs on the growth of intestinal organoids. Including size of

organoids treated with/without HK LGG and EVs, total organoids number and budding organoids percentage of total organoids per well (day 3) (n=50). E. The effects of adding ILC3, ILC3+EVs, ILC3+EVs(LGG)+anti-IL-22, IL-22, IL-22+anti-IL-22 in organoid medium on organoid growth were statistically analyzed (n=50). F: Organoid growth of the experimental group and the control group began to show significant differences on day 2. G: Organoids were stained with EdU (red). Nuclei are stained blue. EdU-positive cells were found in the transit-amplifying region with obvious differences in the percentages among samples (n=10). H: Transcriptional changes of EpCAM, VILLIN, MKI-67, Lgr5, Ascl2, Olfm4, Lyz1 and REG3b genes were detected by q-PCR (n=3).

Fig. 6 | The detection of EVs (LGG) and the pathway of maintaining intestinal immune homeostasis

A: Results of nanoflow cytometry detection of EVs (LGG). B: Observation of EVs (LGG) under electron microscope. C: Detection of EVs (LGG), classification of LGG metabolites in positive and negative ion modes. D: KEGG enrichment analysis was conducted for LGG metabolites. E: The pathway of EVs (LGG) to maintain intestinal immune homeostasis in piglets.

902

903 Fig. S1 | A: The gating of ILC subsets.

904

905 Fig. S2 | A: The statistical analysis of flow cytometry results revealed that antibiotic
906 treatment had an impact on CD4-T cell in LPL, although the difference was not
907 significant. However, it did not have any effect on CD8-T cell. B/C: We showed the
908 results of the correlation analysis between differential metabolites and differential
909 microbial communities, including the positive and negative ion modes. D: UMAP and
910 violin plots showing the AHR was prominently expressed in ILC3 and ILC1 within
911 human intestines. E: UMAP and violin plots showing the AHR was prominently
912 expressed in ILC2 within mice intestines.

913

914 Fig. S3 | A: Immunofluorescence assay showed the expression of LGR5 and Ki-67 in
915 the gut, Analysis by image J software. B: q-PCR experiment counted the secretion of
916 related cytokines in the intestines of piglets in each group. C: Bar chart analysis of the
917 genus-level microbiota in the jejunum of piglets from different groups. D: Heatmap
918 depicting the differences in genus-level microbiota composition in the jejunum of
919 piglets from different groups. E: Alpha diversity refers to the analysis of differences
920 between groups, and box plots can visually represent the median, dispersion,
921 maximum value, minimum value, and outliers of species diversity within each group.
922 F: In the study of beta diversity, four metrics, namely Weighted unifrac distance,
923 Unweighted unifrac distance, Jaccard distance, and Bray-Curtis distance, are used to

924 measure the dissimilarity coefficient between two samples. A smaller value indicates
925 that the two samples have less differences in terms of species diversity.
926
927 Fig. S4 | A: Figure depicting an in vitro co-culture model of ILC3. B: Schematic
928 representation of the flow cytometry gating strategy. C: Illustration of magnetic bead
929 sorting demonstrated by flow cytometry results. D: Proliferation assay of ILC cells,
930 quantitatively analyzed using flow cytometry. E: Schematic diagram of an in vitro
931 co-culture model of ILC3 with IPEC-J2. F: Flow cytometry gating strategy.
932
933 Fig. S5 | A: Growth dynamics of porcine intestinal organoids during 5 days of serial
934 passage culture. B: Schematic representation of the composition of porcine intestinal
935 organoids. C: Immunofluorescence experiment demonstrating the expression of
936 proteins such as Villin, EpCAM, Ki-67, Lgr5, among others, between different groups
937 (n=10).

Figure 1:

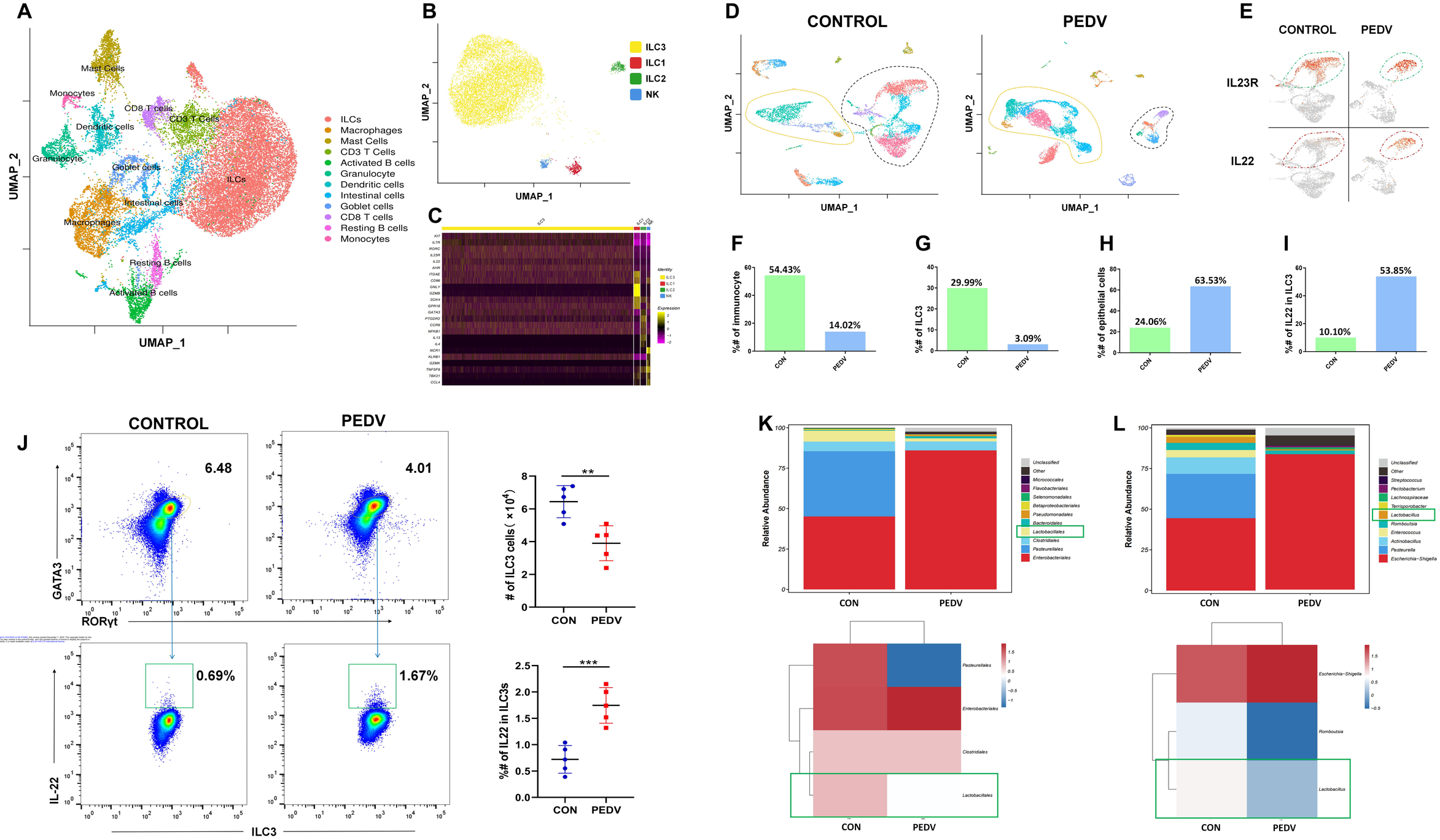
A
Mast Cells
Monocytes
CD8 T cells
CD3 T Cells
Dendritic cells
Granulocyte
Goblet cells
ILCs
Intestinal cells
Macrophages
Resting B cells
Activated B cells
UMAP_2
UMAP_1
ILCs
Macrophages
Mast Cells
CD3 T Cells
Activated B cells
Granulocyte
Dendritic cells
Intestinal cells
Goblet cells
CD8 T cells
Resting B cells
Monocytes
B
ILC3
ILC1
ILC2
NK
UMAP_2
UMAP_1
C
ILC3
ILC1
ILC2
NK
KIT
IL7R
RORC
IL23R
IL22
AHR
ITGAE
CD96
GNLY
GZMB
SOX4
GPR18
GATA3
PTGDR2
CCR6
NFKB1
IL13
IL4
NCR1
KLRB1
GZMK
TNFSF9
TBX21
CCL4
Identity
ILC3
ILC1
ILC2
NK
Expression
2
1
0
−1
−2
D
CONTROL
PEDV
UMAP_2
UMAP_1
UMAP_2
UMAP_1
E
CONTROL
PEDV
IL23R
IL22
F
%# of immunocyte
54.43%
14.02%
CON
PEDV
G
%# of ILC3
29.99%
3.09%
CON
PEDV
H
%# of epithelial cells
24.06%
63.53%
CON
PEDV
I
%# of IL22 in ILC3
10.10%
53.85%
CON
PEDV
J
CONTROL
PEDV
6.48
4.01
GATA3
RORγt
0.69%
1.67%
IL-22
ILC3
# of ILC3 cells(×10^4)
**
CON
PEDV
%# of IL22 in ILC3s
***
CON
PEDV
K
Relative Abundance
CON
PEDV
Unclassified
Other
Micrococcales
Flavobacteriales
Selenomonadales
Betaproteobacteriales
Pseudomonadales
Bacteroidales
Lactobacillales
Clostridiales
Pasteurellales
Enterobacteriales
Pasteurellales
Enterobacteriales
Clostridiales
Lactobacillales
CON
PEDV
L
Relative Abundance
CON
PEDV
Unclassified
Other
Streptococcus
Pectobacterium
Lachnospiraceae
Terrisporobacter
Lactobacillus
Romboutsia
Enterococcus
Actinobacillus
Pasteurella
Escherichia−Shigella
Escherichia−Shigella
Romboutsia
Lactobacillus
CON
PEDV

Figure 2:

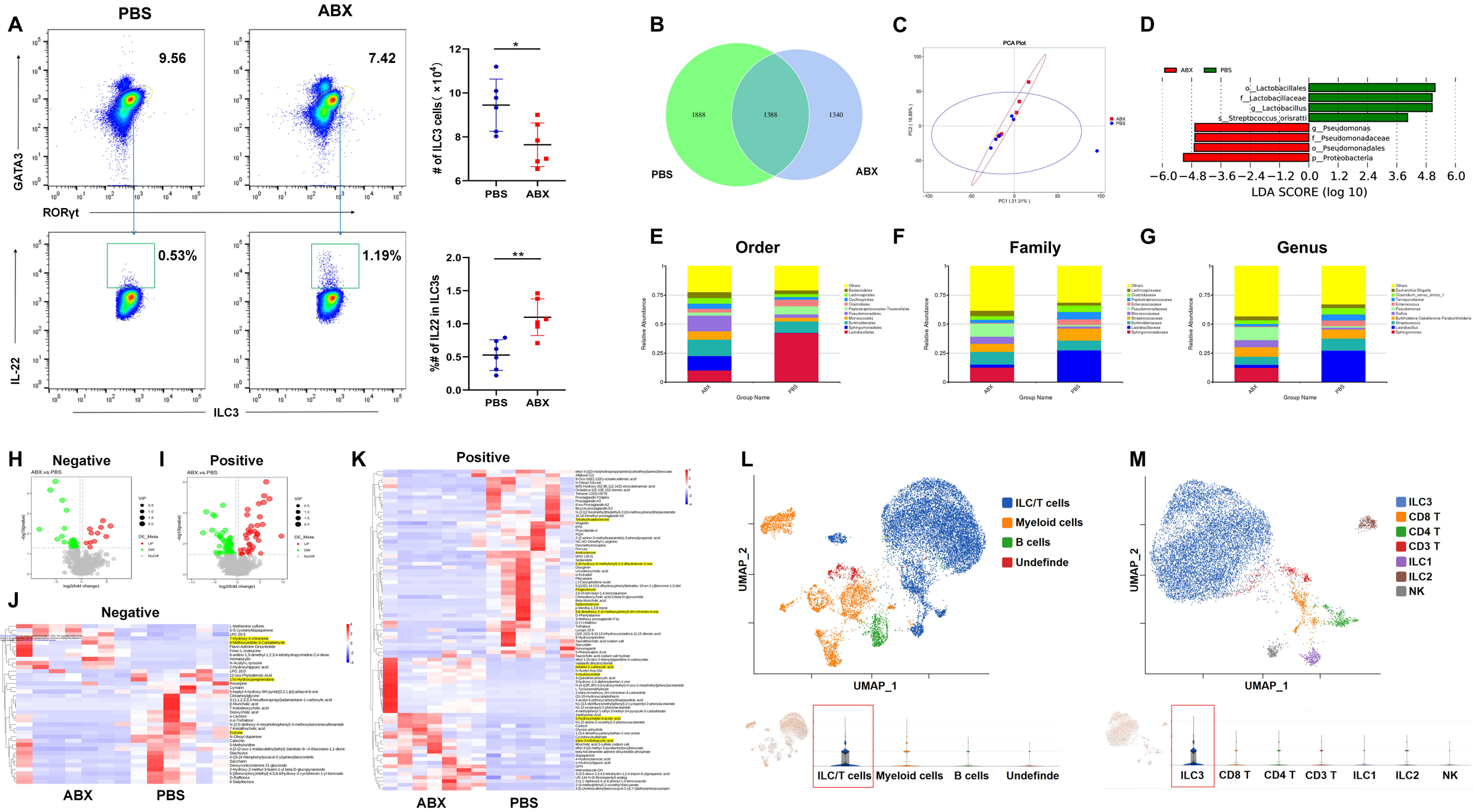
A
PBS
ABX
9.56
7.42
GATA3
RORγt
0.53%
1.19%
IL-22
ILC3
# of ILC3 cells (×10⁴)
%# of IL22 in ILC3s
PBS
ABX
B
1888
1388
1340
C
PCA Plot
PC2 (16.68%)
PC1 (21.31%)
D
o__Lactobacillales
f__Lactobacillaceae
g__Lactobacillus
s__Streptococcus_orisratti
g__Pseudomonas
f__Pseudomonadaceae
o__Pseudomonadales
p__Proteobacteria
LDA SCORE (log 10)
E
Order
F
Family
G
Genus
Relative Abundance
Group Name
H
Negative
I
Positive
ABX.vs.PBS
log2(fold change)
J
Negative
K
Positive
L
ILC/T cells
Myeloid cells
B cells
Undefinde
UMAP_1
UMAP_2
M
ILC3
CD8 T
CD4 T
CD3 T
ILC1
ILC2
NK

Figure 3:

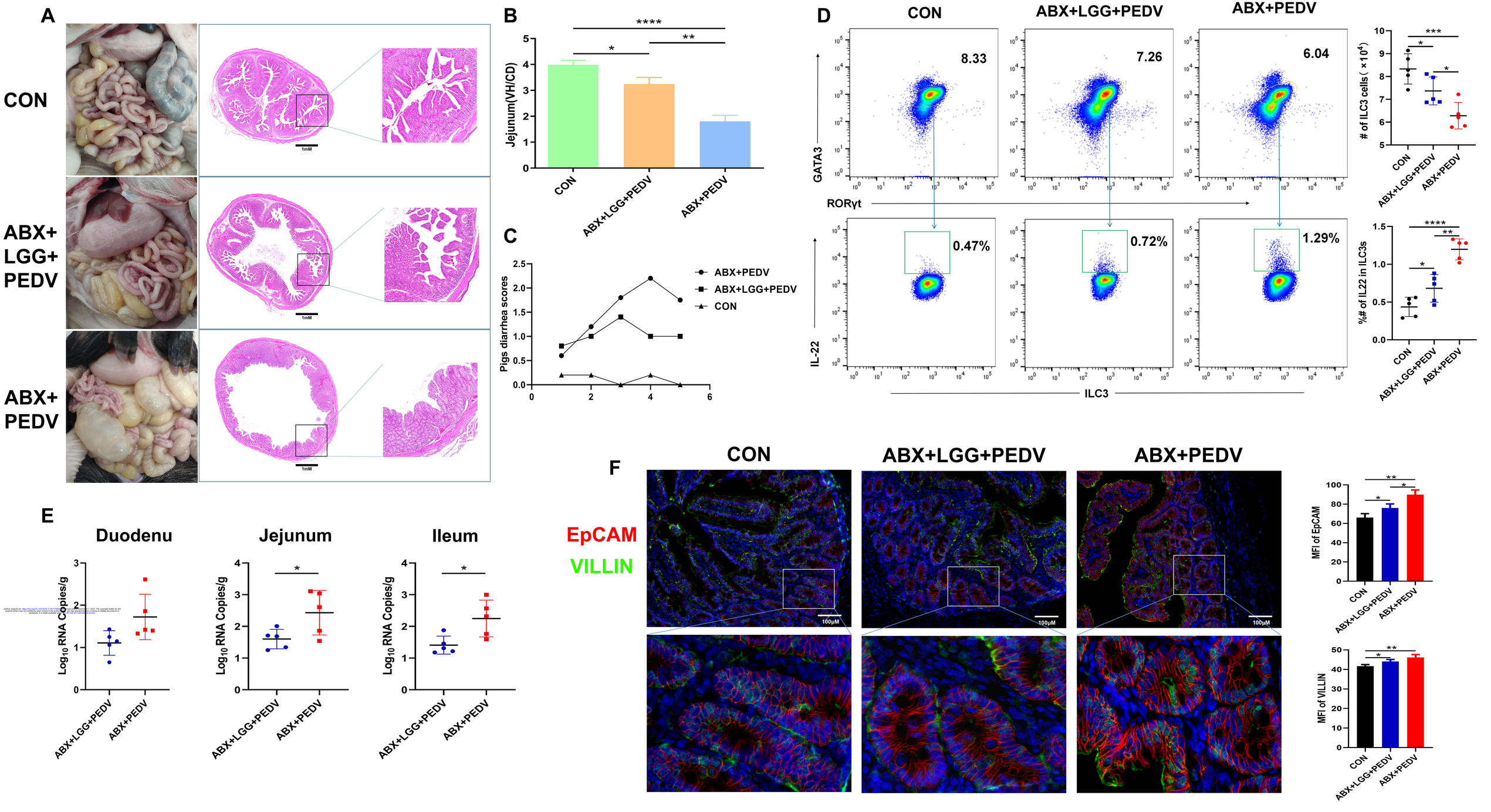
A
CON
ABX+ LGG+ PEDV
ABX+ PEDV
1mM
B
Jejunum(VH/CD)
CON
ABX+LGG+PEDV
ABX+PEDV
C
Pigs diarrhea scores
ABX+PEDV
ABX+LGG+PEDV
CON
D
CON
ABX+LGG+PEDV
ABX+PEDV
GATA3
RORγt
IL-22
ILC3
8.33
7.26
6.04
0.47%
0.72%
1.29%
# of ILC3 cells (×10⁴)
%# of IL22 in ILC3s
E
Duodenu
Jejunum
Ileum
Log10 RNA Copies/g
F
CON
ABX+LGG+PEDV
ABX+PEDV
EpCAM
VILLIN
100μM
MFI of EpCAM
MFI of VILLIN

Figure 4:

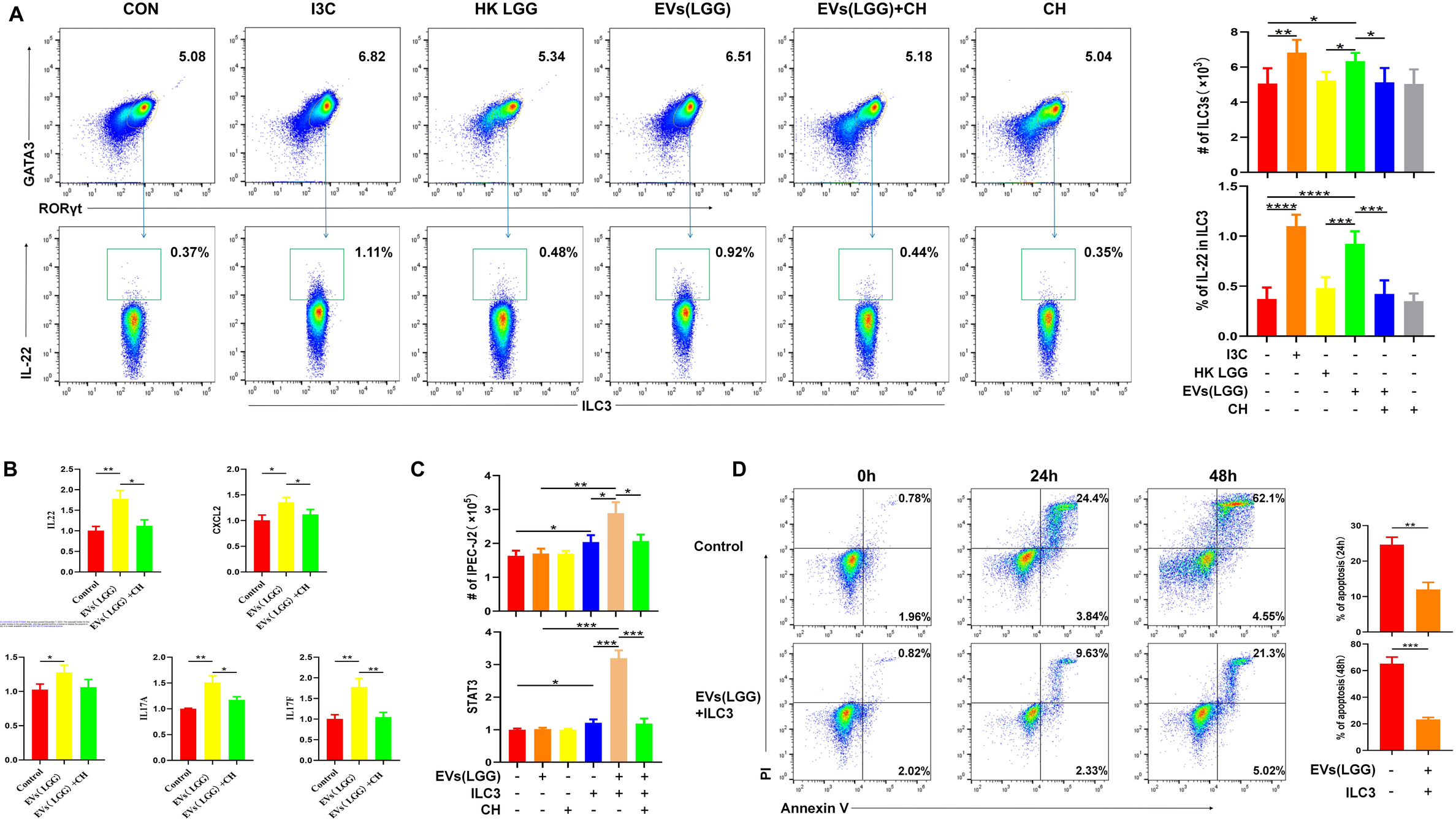
A
CON
I3C
HK LGG
EVs(LGG)
EVs(LGG)+CH
CH
GATA3
RORγt
IL-22
ILC3
5.08
6.82
5.34
6.51
5.18
5.04
0.37%
1.11%
0.48%
0.92%
0.44%
0.35%
# of ILC3s (×10^3)
% of IL-22 in ILC3
I3C
HK LGG
EVs(LGG)
CH
B
IL22
CXCL2
CXCL8
IL17A
IL17F
Control
EVs(LGG)
EVs(LGG)+CH
C
# of IPEC-J2 (×10^5)
STAT3
EVs(LGG)
ILC3
CH
D
0h
24h
48h
Control
EVs(LGG) +ILC3
PI
Annexin V
0.78%
24.4%
62.1%
1.96%
3.84%
4.55%
0.82%
9.63%
21.3%
2.02%
2.33%
5.02%
% of apoptosis (24h)
% of apoptosis (48h)
EVs(LGG)
ILC3

Figure 5:

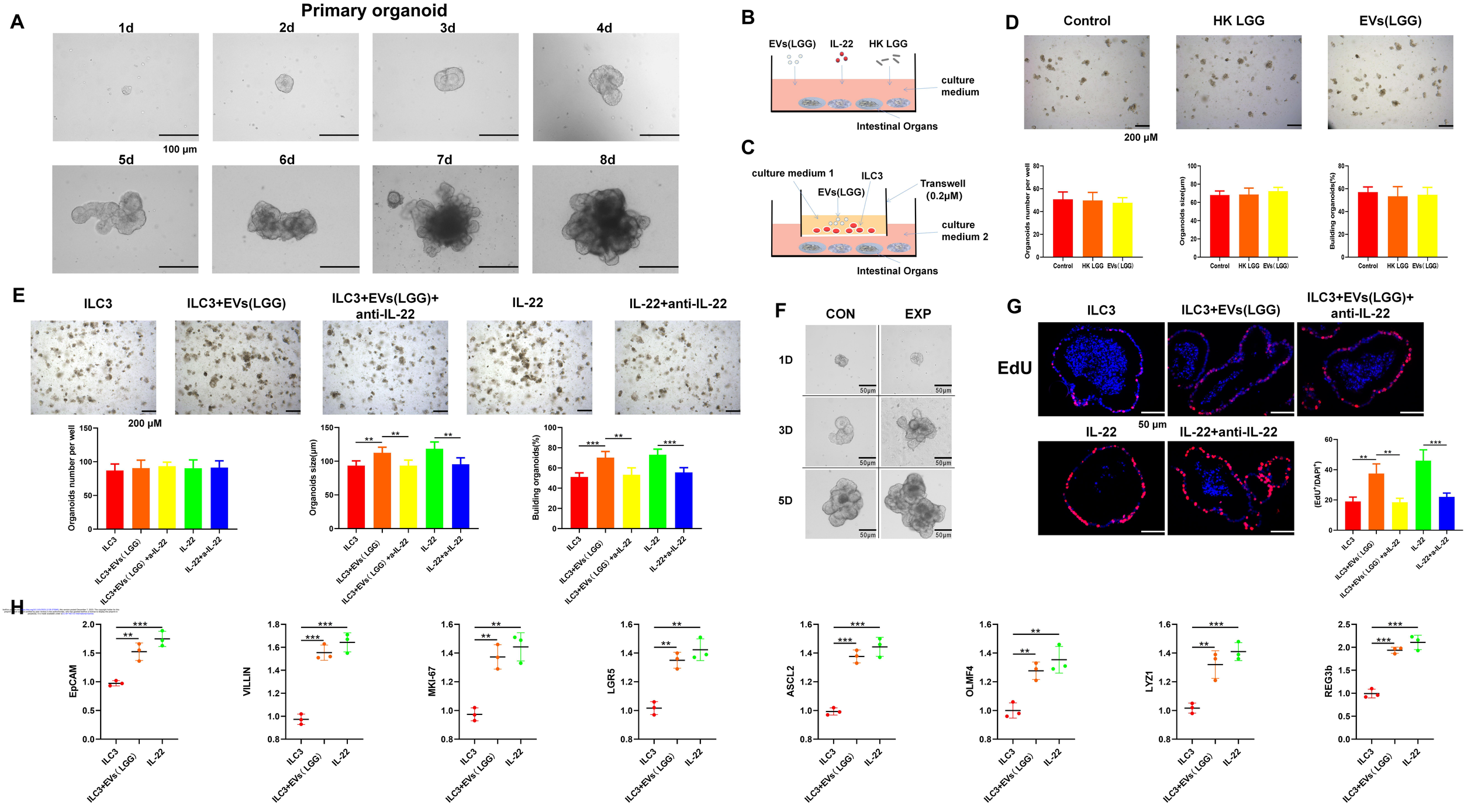
A
Primary organoid
1d
2d
3d
4d
100 μm
5d
6d
7d
8d
B
EVs(LGG)
IL-22
HK LGG
culture medium
Intestinal Organs
C
culture medium 1
ILC3
EVs(LGG)
Transwell (0.2μM)
culture medium 2
Intestinal Organs
D
Control
HK LGG
EVs(LGG)
200 μM
Organoids number per well
Organoids size(μm)
Building organoids(%)
E
ILC3
ILC3+EVs(LGG)
ILC3+EVs(LGG)+ anti-IL-22
IL-22
IL-22+anti-IL-22
200 μM
Organoids number per well
Organoids size(μm)
Building organoids(%)
F
CON
EXP
1D
3D
5D
50μm
G
ILC3
ILC3+EVs(LGG)
ILC3+EVs(LGG)+ anti-IL-22
EdU
50 μm
IL-22
IL-22+anti-IL-22
(EdU+/DAPI+)
H
EpCAM
VILLIN
MKI-67
LGR5
ASCL2
OLMF4
LYZ1
REG3b

Figure 6:

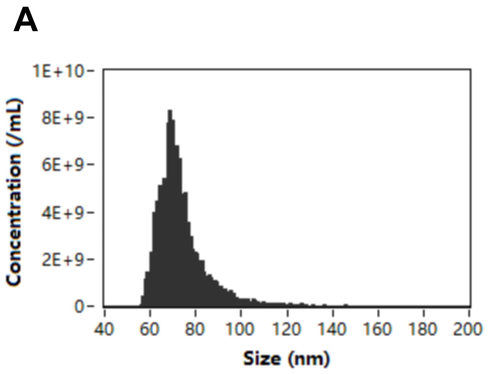

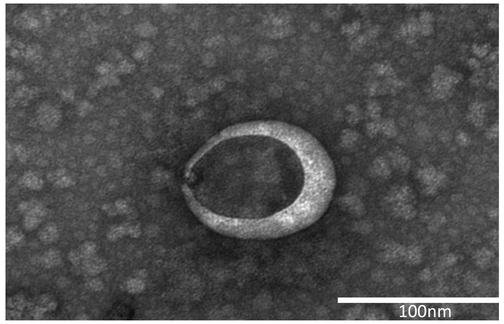

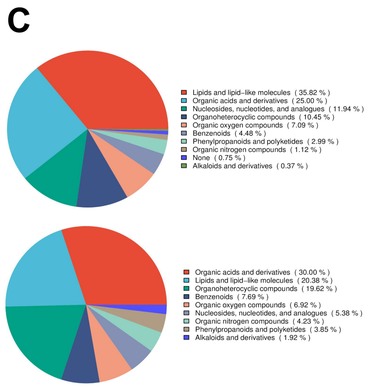

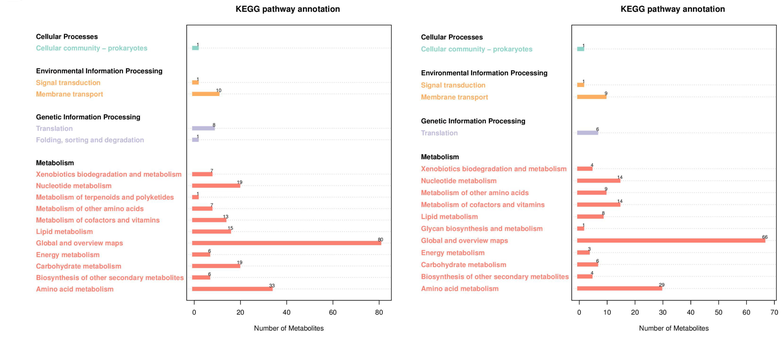

E

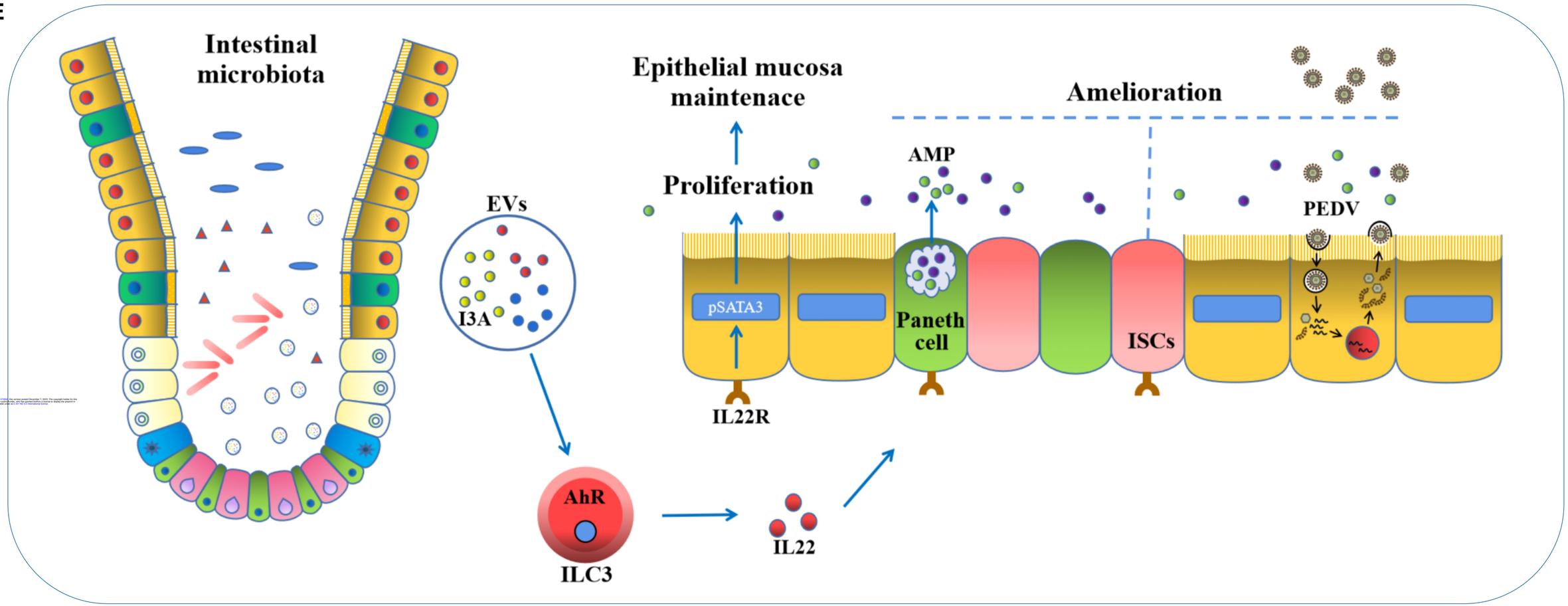

Figure S1:

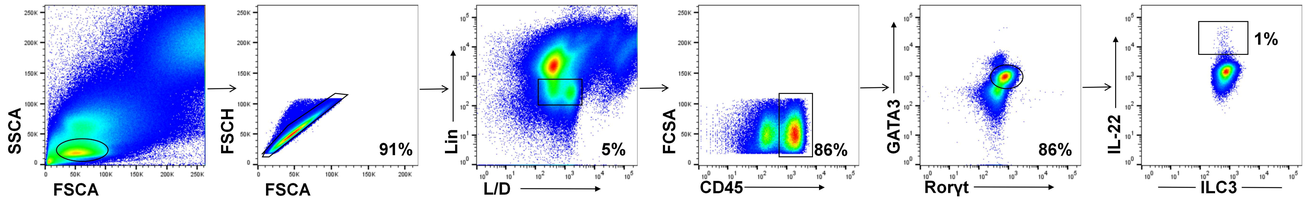

Figure S2：

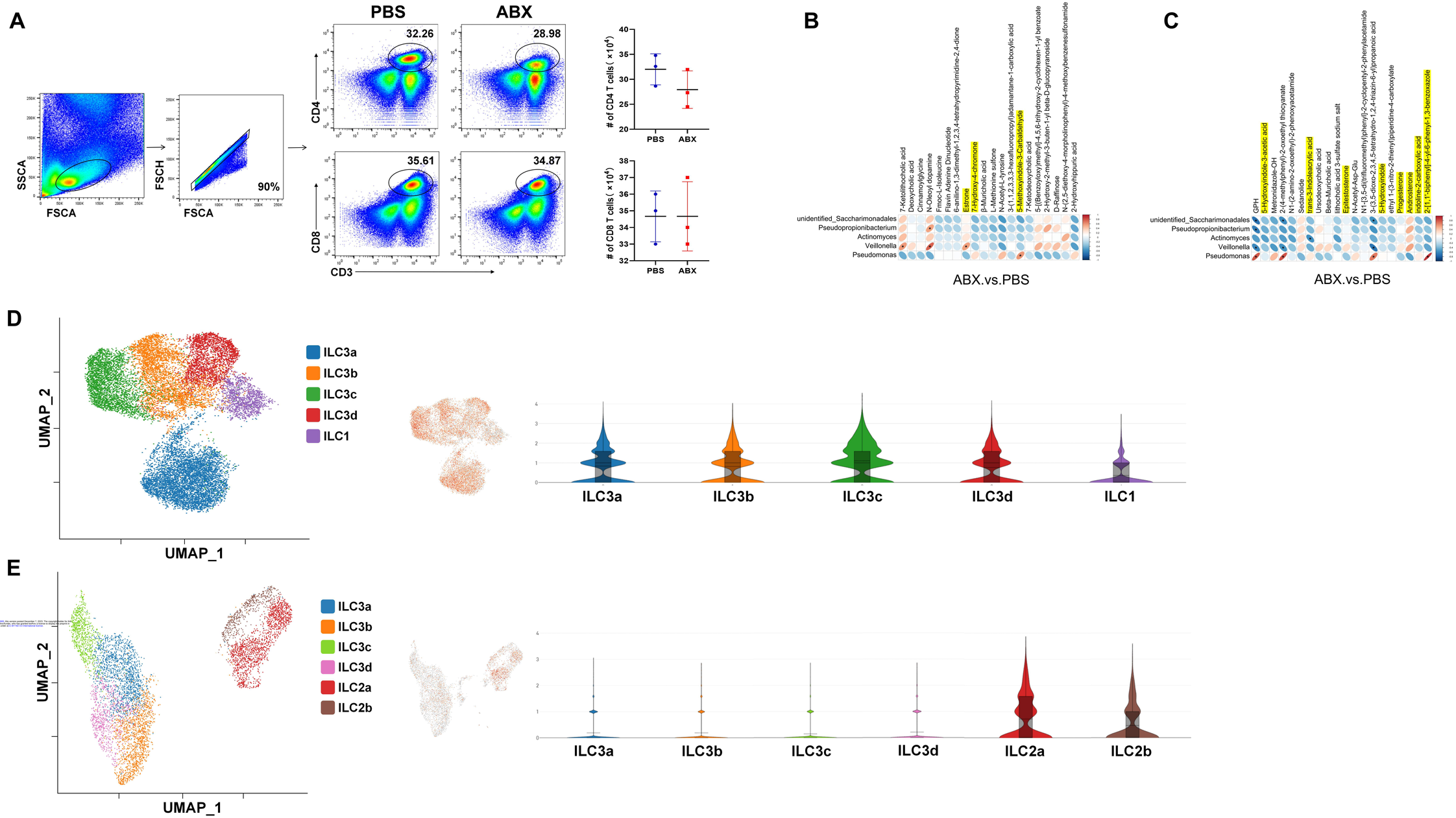
A
PBS
ABX
SSCA
FSCA
FSCH
FSCA
90%
CD4
CD8
CD3
32.26
28.98
35.61
34.87
# of CD4 T cells (×10⁴)
# of CD8 T cells (×10⁴)
PBS
ABX
B
7-Ketolithocholic acid
Deoxycholic acid
Cinnamoylglycine
N-Oleoyl dopamine
Fmoc-L-Isoleucine
Flavin Adenine Dinucleotide
6-anilino-1,3-dimethyl-1,2,3,4-tetrahydropyrimidine-2,4-dione
Estrone
7-Hydroxy-4-chromone
β-Muricholic acid
L-Methionine sulfone
N-Acetyl-L-tyrosine
3-(1,1,2,3,3,3-hexafluoropropyl)adamantane-1-carboxylic acid
5-Methoxyindole-3-Carbaldehyde
7-Ketodeoxycholic acid
5-[(Benzoyloxy)methyl]-4,5,6-trihydroxy-2-cyclohexen-1-yl benzoate
2-Hydroxy-2-methyl-3-buten-1-yl beta-D-glucopyranoside
D-Raffinose
N-(2,5-diethoxy-4-morpholinophenyl)-4-methoxybenzenesulfonamide
2-Hydroxyhippuric acid
unidentified_Saccharimonadales
Pseudopropionibacterium
Actinomyces
Veillonella
Pseudomonas
ABX.vs.PBS
C
GPH
5-Hydroxyindole-3-acetic acid
Metronidazole-OH
2-(4-methylphenyl)-2-oxoethyl thiocyanate
N1-(2-amino-2-oxoethyl)-2-phenoxyacetamide
Sedanolide
trans-3-Indoleacrylic acid
Ursodeoxycholic acid
Beta-Muricholic acid
Ithocholic acid 3-sulfate sodium salt
Epitestosterone
N-Acetyl-Asp-Glu
N1-[3,5-di(trifluoromethyl)phenyl]-2-cyclopentyl-2-phenylacetamide
3-(3,5-dioxo-2,3,4,5-tetrahydro-1,2,4-triazin-6-yl)propanoic acid
5-Hydroxyindole
ethyl 1-(3-nitro-2-thienyl)piperidine-4-carboxylate
Progesterone
Androsterone
Indoline-2-carboxylic acid
2-[1,1'-biphenyl]-4-yl-6-phenyl-1,3-benzoxazole
unidentified_Saccharimonadales
Pseudopropionibacterium
Actinomyces
Veillonella
Pseudomonas
ABX.vs.PBS
D
UMAP_2
UMAP_1
ILC3a
ILC3b
ILC3c
ILC3d
ILC1
ILC3a
ILC3b
ILC3c
ILC3d
ILC1
E
UMAP_2
UMAP_1
ILC3a
ILC3b
ILC3c
ILC3d
ILC2a
ILC2b
ILC3a
ILC3b
ILC3c
ILC3d
ILC2a
ILC2b

Figure s3:

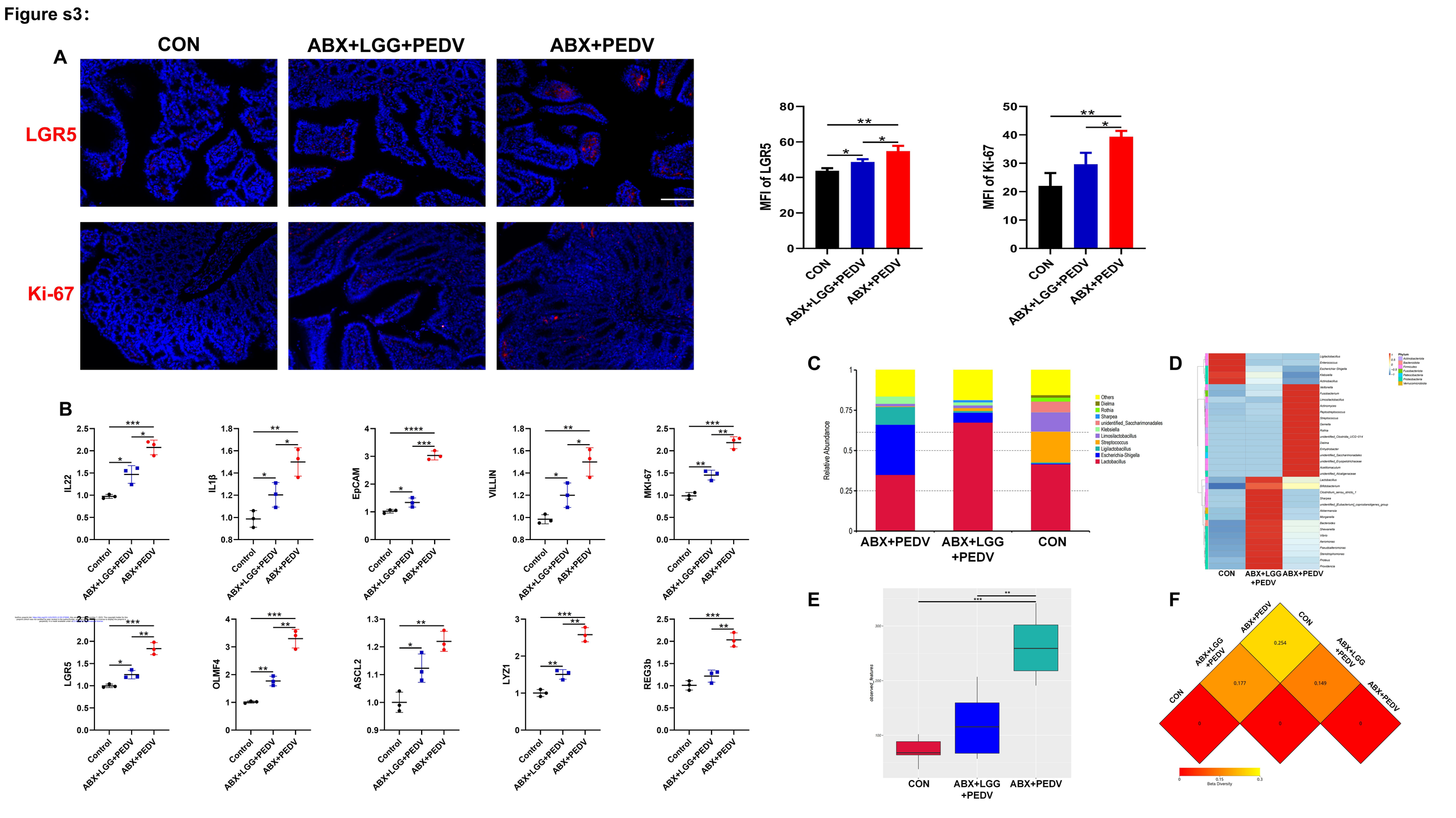
A
CON
ABX+LGG+PEDV
ABX+PEDV
LGR5
Ki-67
MFI of LGR5
MFI of Ki-67
B
IL22
IL1β
EpCAM
VILLIN
MKI-67
LGR5
OLMF4
ASCL2
LYZ1
REG3b
Control
ABX+LGG+PEDV
ABX+PEDV
C
Relative Abundance
Others
Dielma
Rothia
Sharpea
unidentified_Saccharimonadales
Klebsiella
Limosilactobacillus
Streptococcus
Ligilactobacillus
Escherichia-Shigella
Lactobacillus
ABX+PEDV
ABX+LGG +PEDV
CON
D
Phylum
Actinobacteriota
Bacteroidota
Firmicutes
Fusobacteriota
Patescibacteria
Proteobacteria
Verrucomicrobiota
E
observed_features
F
0.254
0.177
0.149
Beta Diversity

Figure s4:

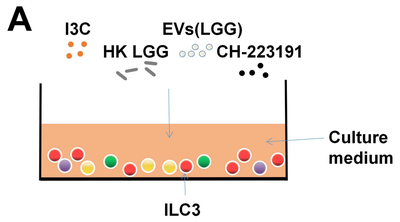

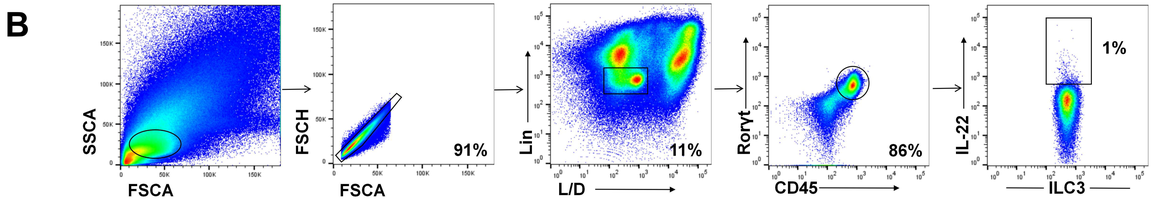

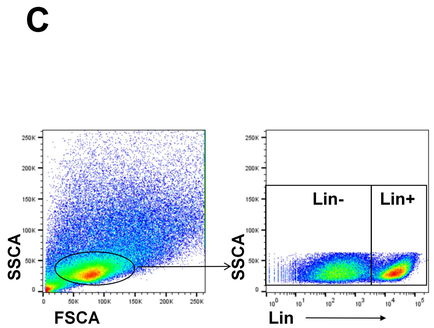

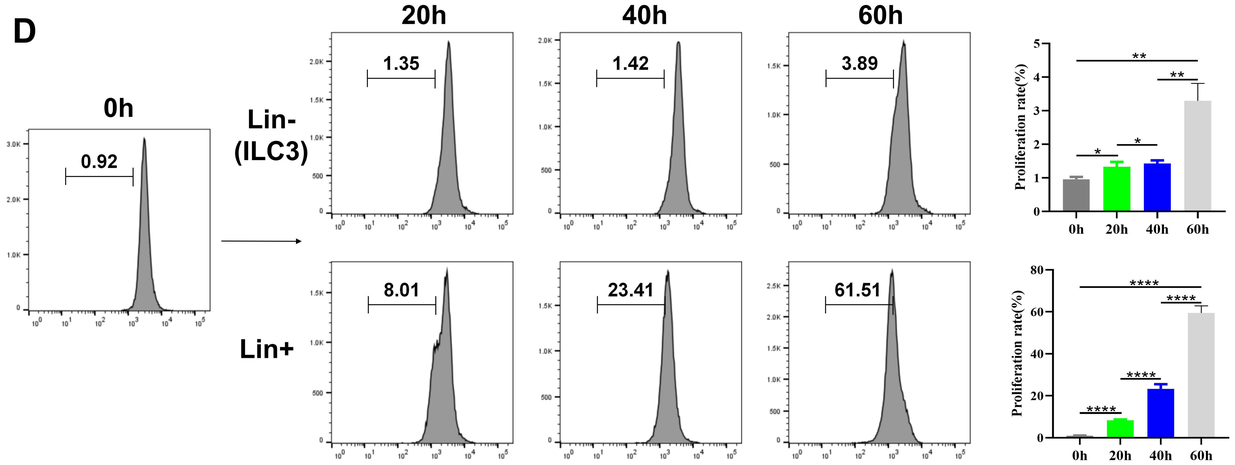

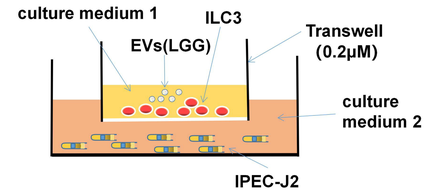

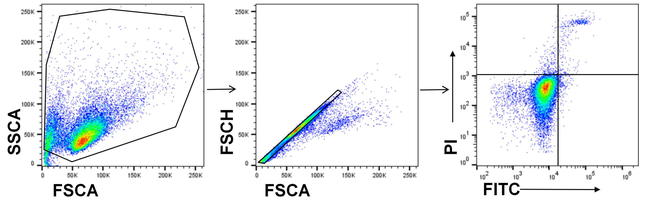

Figure S5:

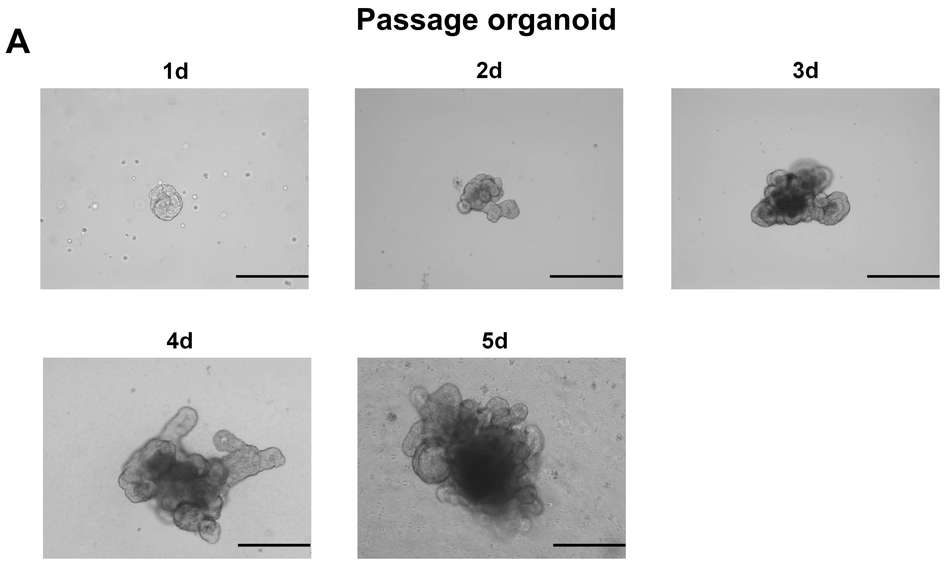
A
Passage organoid
1d
2d
3d
4d
5d

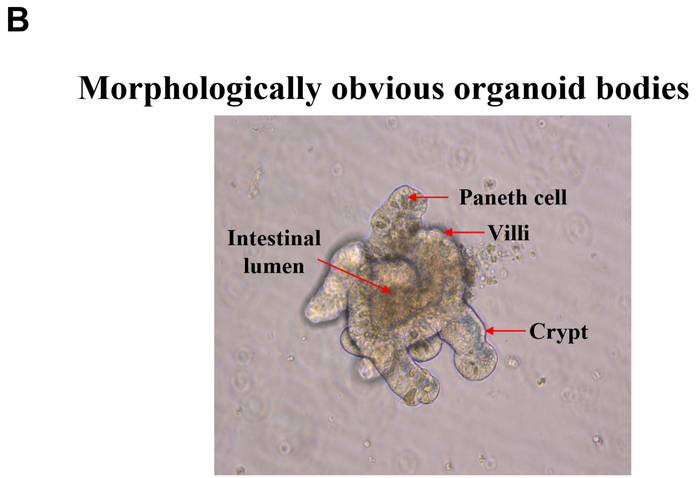
B
Morphologically obvious organoid bodies
Paneth cell
Villi
Intestinal lumen
Crypt

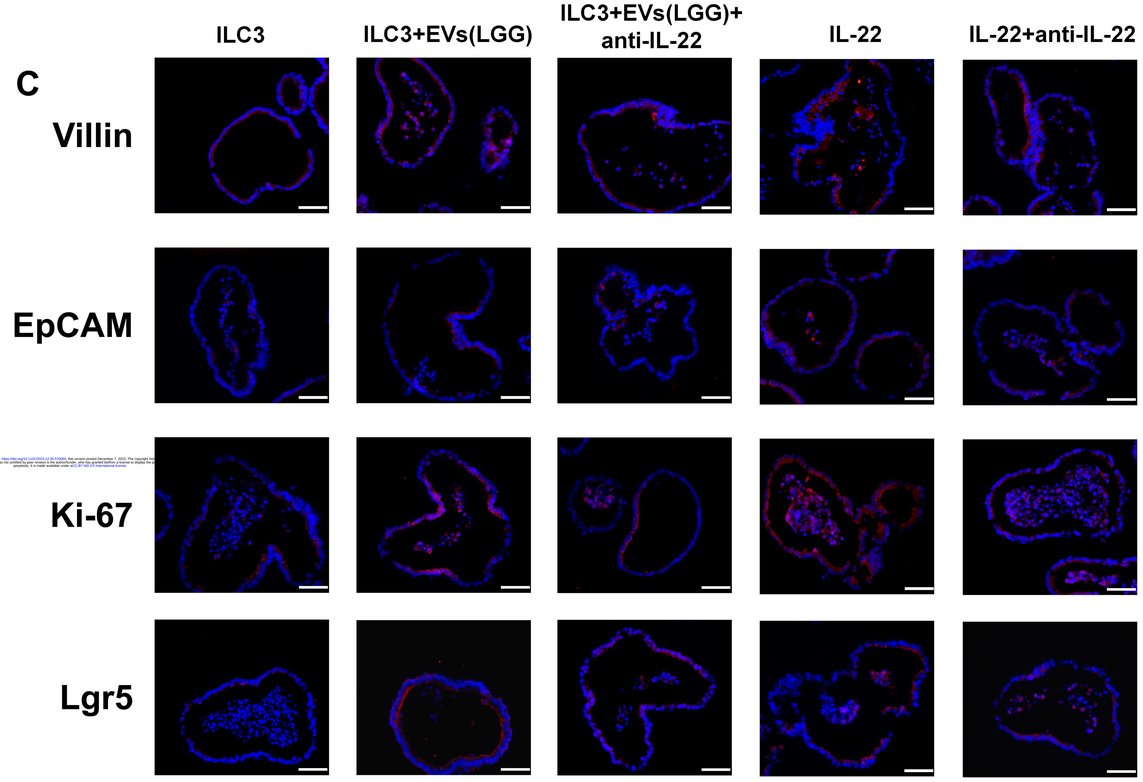
C
ILC3
ILC3+EVs(LGG)
ILC3+EVs(LGG)+ anti-IL-22
IL-22
IL-22+anti-IL-22
Villin
EpCAM
Ki-67
Lgr5

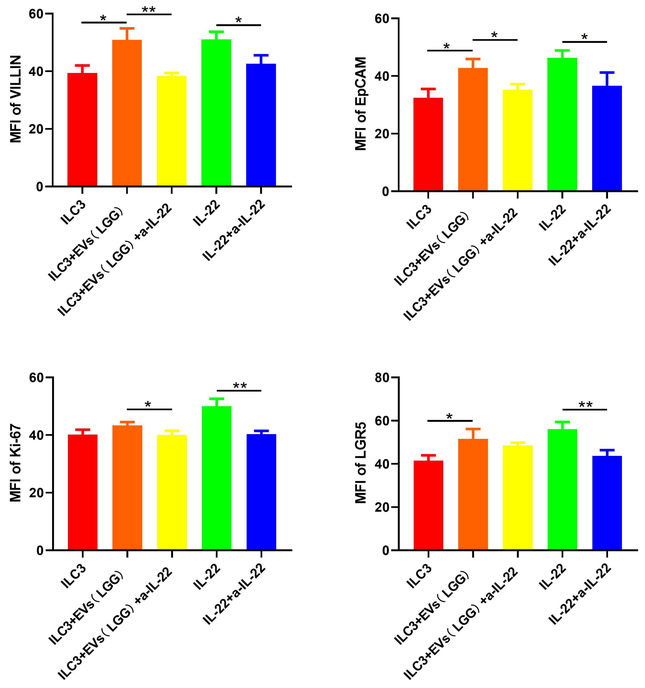
MFI of VILLIN
MFI of EpCAM
MFI of Ki-67
MFI of LGR5
ILC3
ILC3+EVs(LGG)
ILC3+EVs(LGG)+a-IL-22
IL-22
IL-22+a-IL-22